NNLO Results for VV Production

Stefan Kallweit[1]

based on work with: M. Grazzini, D. Rathlev and A. Torre
Phys. Lett. B731 (2014) 204-207 [arXiv:1309.7000 [hep-ph]]

F. Cascioli, T. Gehrmann, M. Grazzini, P. Maierhöfer, A. von Manteuffel, S. Pozzorini, D. Rathlev, L. Tancredi, E. Weihs
Phys.Lett. B735 (2014) 311-313 [arXiv:1405.2219 [hep-ph]]

T. Gehrmann, M. Grazzini, P. Maierhöfer, A. von Manteuffel, S. Pozzorini, D. Rathlev, L. Tancredi
arXiv:1408.5243 [hep-ph] (accepted for publication in PRL)

[1]University of Mainz

October 28–30, 2014, Multi-Boson Interactions Workshop
Brookhaven National Laboratory

Outline

1. Introduction
2. Calculation of NNLO QCD cross sections with q_{T} subtraction
3. Numerical results
   - Inclusive and differential NNLO QCD results for $\mathrm{pp} \to \mathrm{Z}\gamma + \mathrm{X}$
   - Inclusive and differential NNLO QCD results for $\mathrm{pp} \to \mathrm{W}^{\pm}\gamma + \mathrm{X}$
   - Inclusive NNLO QCD results for $\mathrm{pp} \to \mathrm{ZZ} + \mathrm{X}$
   - Inclusive NNLO QCD results for $\mathrm{pp} \to \mathrm{W}^{+}\mathrm{W}^{-} + \mathrm{X}$
4. Conclusions & Outlook

Importance of going beyond NLO in QCD

Fully exclusive NNLO QCD calculations are desirable for several reasons:

- Experimental accuracy has significantly increased, essentially due to LHC, new analysis methods, etc.
- A reduction of the unphysical dependence on factorization and renormalization scales — and in particular reliability of the remaining scale-variation uncertainty as an estimate for missing higher orders — is expected at NNLO.
- In some phase-space regions, NLO is the first non-vanishing order.

  $\hookrightarrow$ Being effectively LO, NLO suffers from typical LO drawbacks.
- In many process classes, all partonic channels are included only from NNLO on.
- Jets are treated more realistically.
- Realistic studies with arbitrary (IR-safe) experimental cuts can be performed.

On the same expected order of magnitude (by naive counting of coupling constants), NLO EW corrections should also be taken into account.

Status of NNLO QCD calculations at hadron colliders – part I

2005

$\mathbf{pp \to H}$ $(m_t \to \infty)$
Sector decomposition
[Anastasiou, Melnikov, Petriello (2005)]

2006

$\mathbf{pp \to V}$
Sector decomposition
[Melnikov, Petriello (2006)]

2007

$\mathbf{pp \to H}$ $(m_t \to \infty)$
q_T subtraction
[Catani, Grazzini (2007)]

2009

$\mathbf{pp \to V}$
q_T subtraction
[Catani, Cieri, Ferrera, de Florian, Grazzini (2009)]

2011

$\mathbf{pp \to WH}$
q_T subtraction
[Ferrera, Grazzini, Tramontano (2011)]

$\mathbf{pp \to \gamma\gamma}$
q_T subtraction
[Catani, Cieri, de Florian, Ferrera, Grazzini (2011)]

2012

$\mathbf{pp \to t\bar{t}}$ ($q\bar{q}$ and gq channels)
STRIPPER (Sector decomposition)
[Bärnreuther, Czakon, Mitov (2012)]

Vector-boson pair production via q_{T} subtraction

The q_{T} subtraction method in its present form is restricted to colourless final states.

↪ The next logical step in this NNLO approach:

Vector-boson pair production pp → VV′ + X

- Important Standard Model test
  ↪ trilinear gauge-boson couplings
- Background for Higgs analyses and BSM searches
- Experimental accuracy is approaching uncertainty of NLO prediction
- Some moderate excesses in the experimental data

	$\sigma\left(\mathrm{pp} \to \mathrm{W^+W^-} + \mathrm{X}\right)$ [pb]	SM NLO [pb]
ATLAS @ 7 TeV	$51.9\,^{+2.0}_{-2.0}\,(\mathrm{stat})\,^{+2.9}_{-2.9}\,(\mathrm{syst})\,^{+2.0}_{-2.0}\,(\mathrm{lumi})$	$47.0\,^{+2.0}_{-1.5}\,(\mathrm{total})$
CMS @ 7 TeV	$52.4\,^{+2.0}_{-2.0}\,(\mathrm{stat})\,^{+4.5}_{-4.5}\,(\mathrm{syst})\,^{+1.2}_{-1.2}\,(\mathrm{lumi})$	
ATLAS @ 8 TeV	$71.4\,^{+1.2}_{-1.2}\,(\mathrm{stat})\,^{+5.0}_{-4.8}\,(\mathrm{syst})\,^{+2.2}_{-2.1}\,(\mathrm{lumi})$	$58.7\,^{+3.0}_{-2.7}\,(\mathrm{total})$
CMS @ 8 TeV	$69.9\,^{+2.8}_{-2.8}\,(\mathrm{stat})\,^{+5.6}_{-5.6}\,(\mathrm{syst})\,^{+3.1}_{-3.1}\,(\mathrm{lumi})$	

Status of NNLO QCD calculations at hadron colliders – part II

2013

$pp \to t\bar{t}$
STRIPPER (Sector decomposition)
[Czakon, Fiedler, Mitov, Rojo (2013)]

$pp \to 2jets$ (gg channel)
Antenna subtraction (leading colour)
[Gehrmann-De Ridder, Gehrmann, Glover, Pires (2013)]

$pp \to 2jets$ (gg channel)
Colourful antenna subtraction
[Currie, Gehrmann-De Ridder, Glover, Pires (2013)]

$pp \to H + jet$ (gg channel)
Sector decomposition
[Boughezal, Caola, Melnikov, Petriello, Schulze (2013)]

$pp \to HH$ ($m_t \to \infty$)
$pp \to H$ + FKS subtraction
[de Florian, Mazzitelli (2013)]

$pp \to Z\gamma$
q_T subtraction
[Grazzini, SK, Rathlev, Torre (2013)]

[$pp \to W\gamma$]
q_T subtraction
[Grazzini, SK, Rathlev, Torre (to be published...)]

2014

$pp \to t/\bar{t} + jet$
Sector decomposition
[Brucherseifer, Caola, Melnikov (2014)]

$pp \to t\bar{t}$ ($q\bar{q}$ channels)
Antenna subtraction (leading colour)
[Abelof, Gehrmann-De Ridder, Maierhöfer, Pozzorini (2014)]

$pp \to ZZ$
q_T subtraction
[Cascioli, Gehrmann, Grazzini, SK, Maierhöfer, von Manteuffel, Pozzorini, Rathlev, Tancredi, Weihs (2014)]

$pp \to WW$
q_T subtraction
[Gehrmann, Grazzini, SK, Maierhöfer, von Manteuffel, Pozzorini, Rathlev, Tancredi (2014)]

Sketchy presentation of the q_T subtraction method

- Consider the production of a colourless final state F via $\mathbf{q\bar{q} \to F}$, or $\mathbf{gg \to F}$:

$$\mathrm{d}\sigma_{\mathrm{F}}^{(\mathrm{N})\mathrm{NLO}}\Big|_{q_T \neq 0} = \mathrm{d}\sigma_{\mathrm{F+jet}}^{(\mathrm{N})\mathrm{LO}},$$

  where q_T refers to the transverse momentum of the colourless system F.

- $\mathrm{d}\sigma_{\mathrm{F}}^{(\mathrm{N})\mathrm{NLO}}\Big|_{q_T \neq 0}$ is singular for $q_T \to 0$, but the limiting behaviour is known from transverse momentum resummation.
  [Bozzi, Catani, de Florian, Grazzini (2006)]

Sketchy presentation of the q_T subtraction method

- Consider the production of a colourless final state F via $\mathbf{q\bar{q} \to F}$, or $\mathbf{gg \to F}$:

$$\mathrm{d}\sigma_{\mathrm{F}}^{(\mathrm{N})\mathrm{NLO}}\Big|_{q_{\mathrm{T}}\neq 0} = \mathrm{d}\sigma_{\mathrm{F+jet}}^{(\mathrm{N})\mathrm{LO}},$$

  where q_T refers to the transverse momentum of the colourless system F.

- $\mathrm{d}\sigma_{\mathrm{F}}^{(\mathrm{N})\mathrm{NLO}}\Big|_{q_{\mathrm{T}}\neq 0}$ is singular for $q_T \to 0$, but the limiting behaviour is known from transverse momentum resummation.
  [Bozzi, Catani, de Florian, Grazzini (2006)]

- Define a counterterm,

$$\mathrm{d}\sigma^{\mathrm{CT}} = \Sigma(q_{\mathrm{T}}/Q) \otimes \mathrm{d}\sigma^{\mathrm{LO}}, \quad Q \equiv m_{\mathrm{F}},$$

  which has the same limiting behaviour for $q_T \to 0$.

- Add the $q_T = 0$ piece to obtain the full result:

$$\mathrm{d}\sigma_{\mathrm{F}}^{(\mathrm{N})\mathrm{NLO}} = \mathcal{H}_{\mathrm{F}}^{(\mathrm{N})\mathrm{NLO}} \otimes \mathrm{d}\sigma^{\mathrm{LO}} + \left[\mathrm{d}\sigma_{\mathrm{F+jet}}^{(\mathrm{N})\mathrm{LO}} - \Sigma \otimes \mathrm{d}\sigma^{\mathrm{LO}}\right]$$

Ingredients of the q_T subtraction method

$$\mathrm{d}\sigma_{\mathrm{F}}^{(\mathrm{N})\mathrm{NLO}} = \mathcal{H}_{\mathrm{F}}^{(\mathrm{N})\mathrm{NLO}} \otimes \mathrm{d}\sigma^{\mathrm{LO}} + \left[\mathrm{d}\sigma_{\mathrm{F+jet}}^{(\mathrm{N})\mathrm{LO}} - \Sigma \otimes \mathrm{d}\sigma^{\mathrm{LO}}\right]$$

- The hard–virtual coefficients,

$$\mathcal{H}_{\mathrm{F}} = \underbrace{1}_{\substack{\text{tree-level}\\ \text{amplitude}}} + \underbrace{\left(\frac{\alpha_S}{\pi}\right)\mathcal{H}^{\mathrm{F}(1)}}_{\substack{\text{contains (finite)}\\ \text{1-loop amplitude}}} + \underbrace{\left(\frac{\alpha_S}{\pi}\right)^2\mathcal{H}^{\mathrm{F}(2)}}_{\substack{\text{contains (finite)}\\ \text{2-loop amplitude}}} + \ldots,$$

  are known up to 2-loop order by means of a process-independent extraction procedure, starting from the all-order virtual amplitude of the specific process.
  [Catani, Cieri, de Florian, Ferrera, Grazzini (2013)]

- $\mathrm{d}\sigma_{\mathrm{F+jets}}^{\mathrm{NLO}}$ can be treated by well-known NLO subtraction techniques.

- The counterterm

$$\Sigma(q_T/Q) = \left(\frac{\alpha_S}{\pi}\right)\Sigma^{(1)}(q_T/Q) + \left(\frac{\alpha_S}{\pi}\right)^2\Sigma^{(2)}(q_T/Q) + \ldots$$

  is universal (differs for $\mathrm{q\bar{q}} \to \mathrm{F}$ and $\mathrm{gg} \to \mathrm{F}$, trivial process dependence), and the coefficients are known (up to 2-loop order).
  [Bozzi, Catani, de Florian, Grazzini (2006)]

Technical ingredients of the calculation

Scattering amplitudes up to 1-loop with OpenLoops [Cascioli, Maierhöfer, Pozzorini (2011)]

- Tree, one-loop and real-emission amplitudes (including colour/helicity correlations)
- Fully automated for NLO QCD for any SM process
- Provides also finite (1-loop)-squared amplitudes (not only)
- Compact and fast numerical code

Tensor reduction by means of the Collier library [Denner, Dittmaier, Hofer (to be published)]

- Numerically stable Denner–Dittmaier reduction methods [Denner, Dittmaier (2002 & 2005)]
- Scalar integrals with complex masses [Denner, Dittmaier (2010)]

Rescue system by quad-precision CutTools for critical points [Ossola, Papadopoulos, Pittau (2008)]

- Scalar integrals from OneLOop [van Hameren, Papadopoulos, Pittau (2009)]; van Hameren (2010)]

2-loop amplitudes from analytic results [Matsuura, van der Marck, van Neerven (1989); Gehrmann, Tancredi (2011); [Gehrmann, von Manteuffel, Tancredi, Weihs (2013 & 2014); Gehrmann, von Manteuffel, Tancredi (to be published)]

- Numerical implementation using GiNaC [Bauer, Frink, Kreckel (2002) + Kisil, Sheplyakov, Vollinga, ...]

Mediation of IR divergences between phase-spaces

- Dipole subtraction for massless particles in NLO parts [Catani, Seymour (1993)]
- q_T subtraction for dealing with the remaining singularities.

Numerical realization of the calculation

Fully automated NLO QCD Monte Carlo framework [SK]
(implementation in C++)

- Phase-space integration by multi-channel Monte Carlo techniques:
  - Automatized generation of mappings for arbitrary partonic processes
  - Additional Monte Carlo channels based on dipole kinematics
    (improvement of convergence, particularly in multi-resonance processes)

$\hookrightarrow$ Fast and stable numeric calculation of cross sections and distributions.

Numerical realization of the calculation

Fully automated NLO QCD Monte Carlo framework [SK]
(implementation in C++)

- Phase-space integration by multi-channel Monte Carlo techniques:
  - Automatized generation of mappings for arbitrary partonic processes
  - Additional Monte Carlo channels based on dipole kinematics
    (improvement of convergence, particularly in multi-resonance processes)

  ↪ Fast and stable numeric calculation of cross sections and distributions.

- Additional features of the integrator:
  - Code generation for arbitrary Standard Model process
    (including automatic bookkeeping of all required partonic channels)
  - Automatic generation of OpenLoops interface
  - Automatic selection and construction of massless and massive dipoles
  - Simultaneous calculations for different scale choices and variations

↪ All ingredients well tested in various multi-particle processes!

Extension to NLO EW implemented and ready for applications!

Numerical implementation of the calculation

Extension to automated (q_{T} subtraction) NNLO QCD framework [SK, Rathlev]

- Implementation of additional contributions needed in q_{T} subtraction:
  - $\mathrm{cut}_{q_{\mathrm{T}}/q}$-dependent counterterm contribution with numerical integration over q_{T}
  - $\mathrm{cut}_{q_{\mathrm{T}}/q}$-independent hard–collinear coefficients
    $\hookrightarrow$ both contain non-trivial pdf factors (single and double collinear emission)
  - Extra-jet-emission part with extremely low $\mathrm{cut}_{q_{\mathrm{T}}/q}$.

Numerical implementation of the calculation

Extension to automated (q_{T} subtraction) NNLO QCD framework [SK, Rathlev]

- Implementation of additional contributions needed in q_{T} subtraction:
  - $\mathrm{cut}_{q_{\mathrm{T}}/q}$-dependent counterterm contribution with numerical integration over q_{T}
  - $\mathrm{cut}_{q_{\mathrm{T}}/q}$-independent hard–collinear coefficients
    $\hookrightarrow$ both contain non-trivial pdf factors (single and double collinear emission)
  - Extra-jet-emission part with extremely low $\mathrm{cut}_{q_{\mathrm{T}}/q}$.
- Highly efficient integration, particularly of $\mathrm{cut}_{q_{\mathrm{T}}/q}$-dependent parts, required:
  - Importance sampling on top of usual parametrization of phase-space variables (particularly relevant for t-channel propagators related to jet emission).
  - Improved implementation of $(K + P)$ terms (Catani–Seymour) to avoid contributions from different phase-spaces (mis-binning/spoilt cancellations).
  - Initial-state multi channelling to account e. g. for $V \to \mathrm{l\bar{l}}\gamma$ contribution (not a peculiar NNLO issue).

Numerical implementation of the calculation

Extension to automated (q_T subtraction) NNLO QCD framework [SK, Rathlev]

- Implementation of additional contributions needed in q_T subtraction:
  - $\mathrm{cut}_{q_T/q}$-dependent counterterm contribution with numerical integration over q_T
  - $\mathrm{cut}_{q_T/q}$-independent hard–collinear coefficients
    $\hookrightarrow$ both contain non-trivial pdf factors (single and double collinear emission)
  - Extra-jet-emission part with extremely low $\mathrm{cut}_{q_T/q}$.
- Highly efficient integration, particularly of $\mathrm{cut}_{q_T/q}$-dependent parts, required:
  - Importance sampling on top of usual parametrization of phase-space variables (particularly relevant for t-channel propagators related to jet emission).
  - Improved implementation of $(K + P)$ terms (Catani–Seymour) to avoid contributions from different phase-spaces (mis-binning/spoilt cancellations).
  - Initial-state multi channelling to account e. g. for $V \to l\bar{l}\gamma$ contribution (not a peculiar NNLO issue).
- Simultaneous evaluation of observables for different values of the regulator $\mathrm{cut}_{q_T/q}$
  $\hookrightarrow$ provides numerical check of $\mathrm{cut}_{q_T/q}$ dependence.

$\hookrightarrow$ Applicability to NNLO calculations (based on q_T subtraction) proven!

Expertise for all ingredients crucial for VV @ NNLO QCD

Numerical results for $\mathrm{pp} \to \mathrm{Z}\gamma + \mathrm{X}$ at NNLO QCD

Numerical setups for $Z\gamma$ production

(Central) scale choice: $\mu_R = \mu_F = \mu_0 \equiv \sqrt{m_Z^2 + p_{\gamma,T}^2}$.

Setup of the ATLAS analysis @ 7 TeV
[ATLAS collaboration (2013)]

- $p_{\gamma,T} > 15\,\text{GeV}$ or $p_{\gamma,T} > 40\,\text{GeV}$
- $|\eta_\gamma| < 2.37$
- $p_{l^\pm,T} > 25\,\text{GeV}$
- $|\eta_{l^\pm}| < 2.47$
- $m_{l^-l^+} > 40\,\text{GeV}$
- $\Delta R(l^\pm, \gamma) > 0.7$
- Smooth cone isolation [Frixione (1998)] with $n = 1$, $\delta_0 = 0.4$, and $\varepsilon = 0.5$
- Anti-k_T algorithm with $D = 0.4$
  $\hookrightarrow E_{\text{jet},T} > 30\,\text{GeV}$, $|\eta_{\text{jet}}| < 4.4$
- $\Delta R(l^\pm/\gamma, jet) > 0.3$

Setup of the CMS analysis @ 7 TeV
[CMS collaboration (2013)]

- $p_{\gamma,T} > 15\,\text{GeV}$
- $|\eta_\gamma| < 2.5$
- $p_{l^\pm,T} > 20\,\text{GeV}$
- $|\eta_{l^\pm}| < 2.5$
- $m_{l^-l^+} > 50\,\text{GeV}$
- $\Delta R(l^\pm, \gamma) > 0.7$
- Smooth cone isolation [Frixione (1998)] with $n = 1$, $\delta_0 = 0.3$, and $\varepsilon = 0.05$

Further setups under invesigation:

- ATLAS and CMS setups @ 8 TeV
- LHCb setup @ 8 TeV
  (asymmetric forward kinematics)

Dependence on q_T (LHC @ 7 TeV, ATLAS setup, $p_{T,\gamma} > 40\,\mathrm{GeV}$)

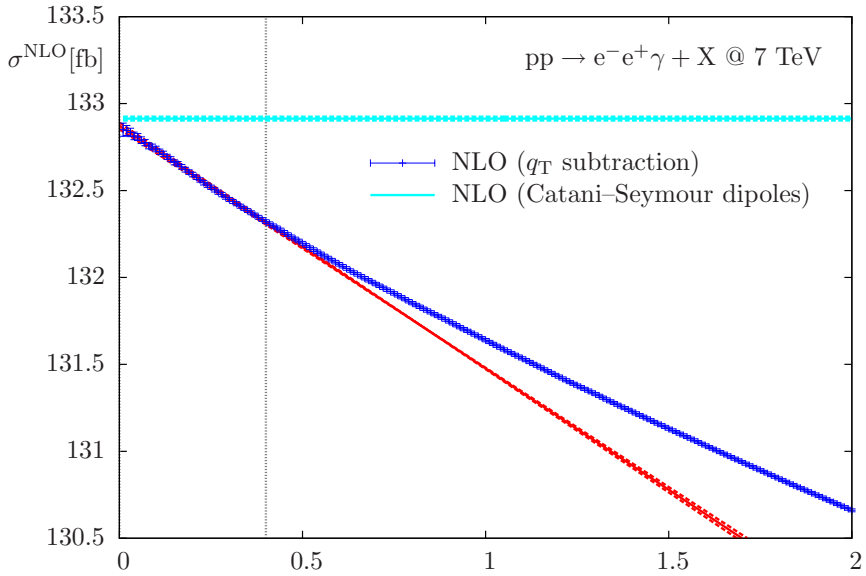

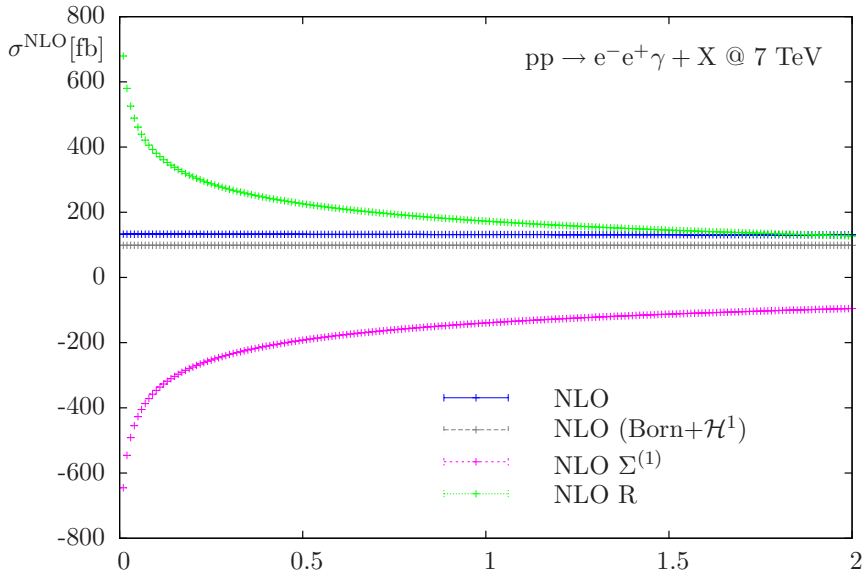

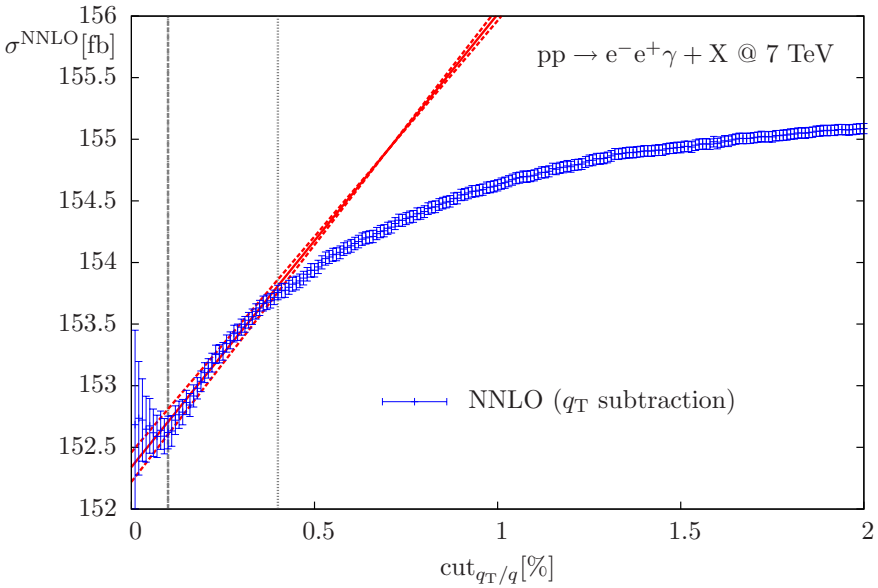

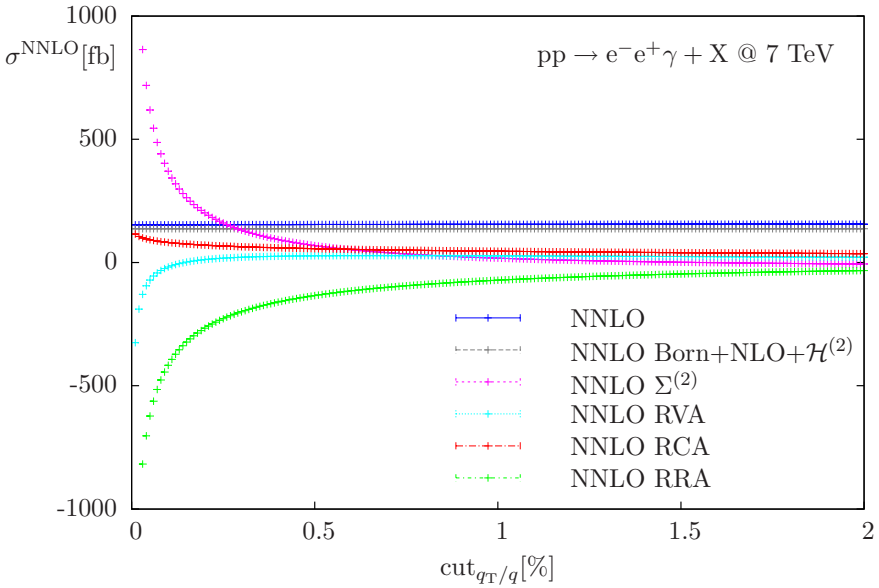

Scale variation (LHC @ 7 TeV, ATLAS setup, $p_{\mathrm{T},\gamma} > 15\,\mathrm{GeV}$)

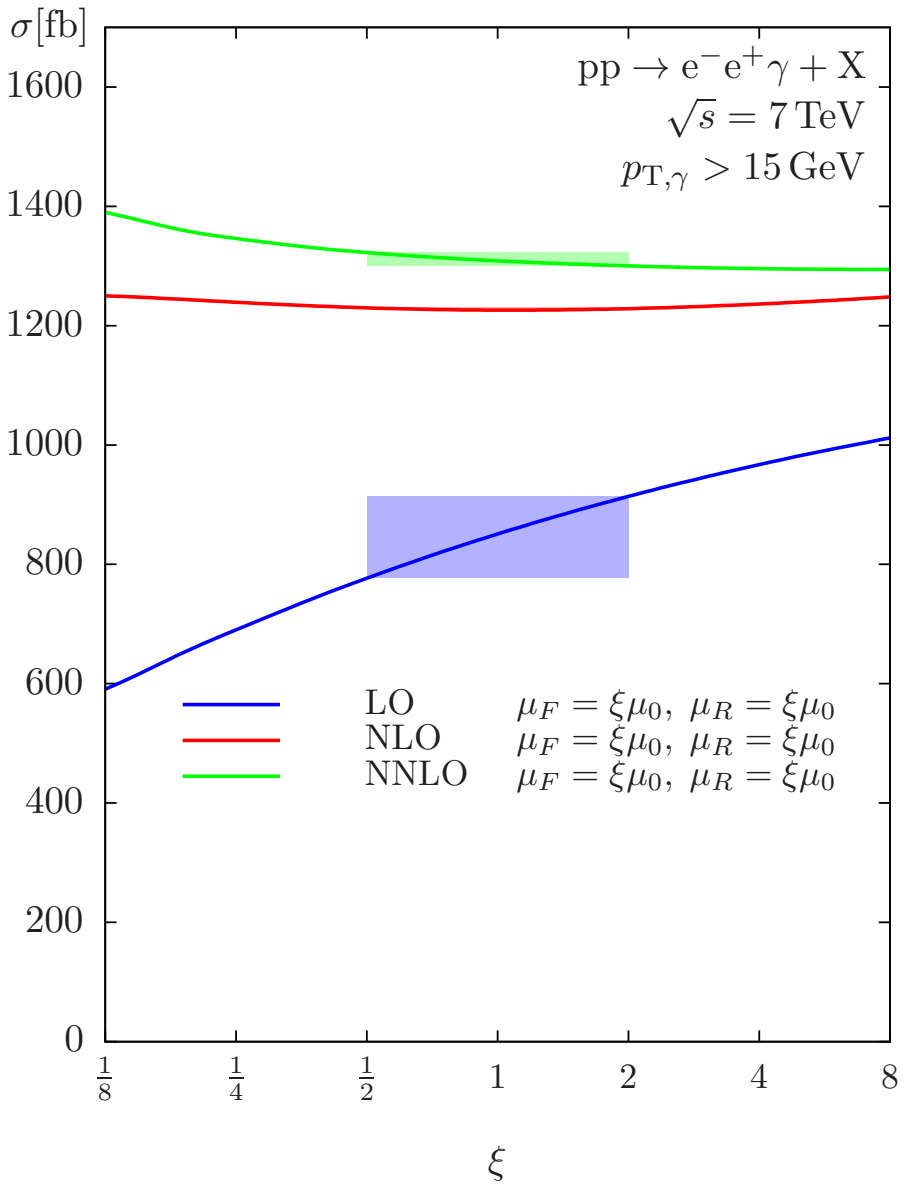

- Scale variation essentially disappears at NLO and NNLO if variation with $\mu_{\mathrm{F}} = \mu_{\mathrm{R}}$ is considered.

  $\hookrightarrow$ accidental cancellation between μ_{F} and μ_{R} dependence!

Scale variation (LHC @ 7 TeV, ATLAS setup, $p_{\mathrm{T},\gamma} > 15\,\mathrm{GeV}$)

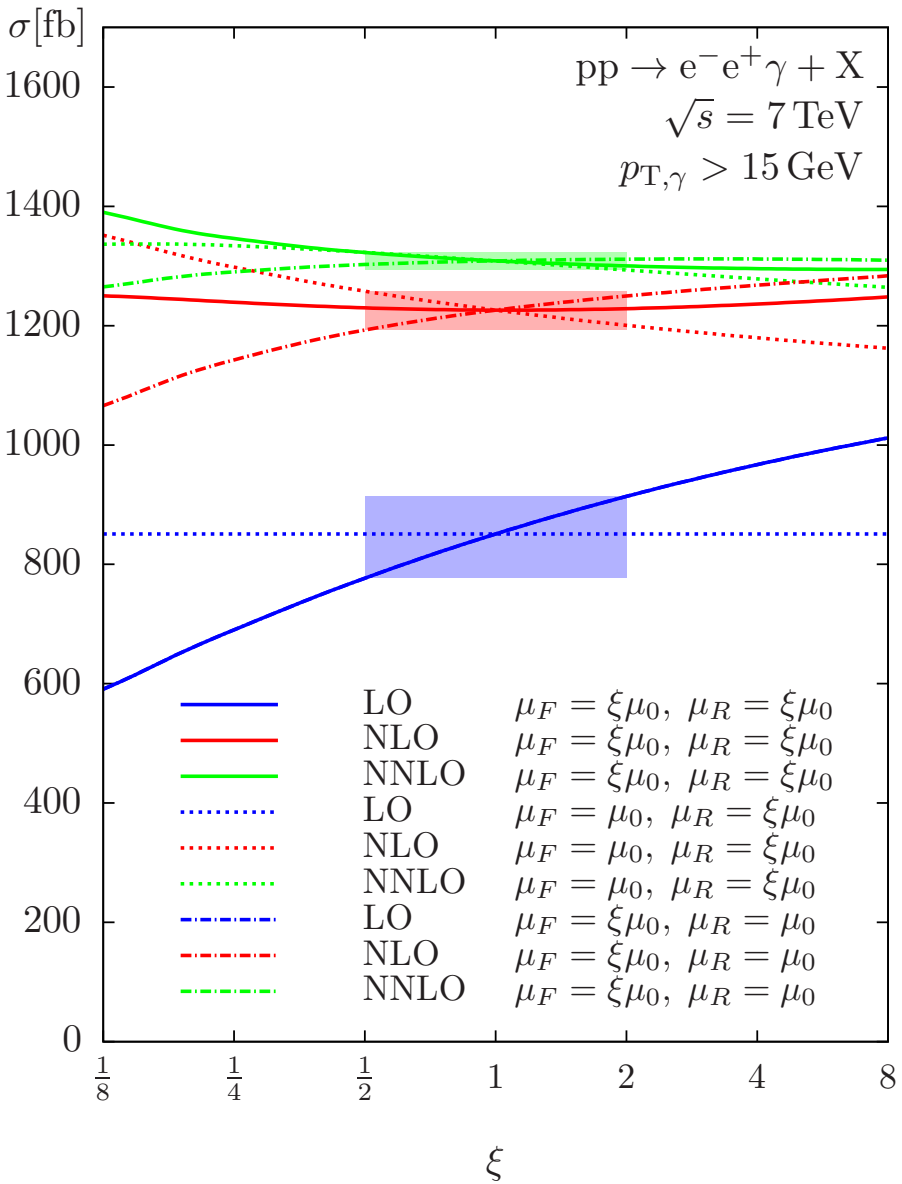

- Scale variation essentially disappears at NLO and NNLO if variation with $\mu_{\mathrm{F}} = \mu_{\mathrm{R}}$ is considered.

  $\hookrightarrow$ accidental cancellation between μ_{F} and μ_{R} dependence!

Scale variation (LHC @ 7 TeV, ATLAS setup, $p_{T,\gamma} > 15\,\mathrm{GeV}$)

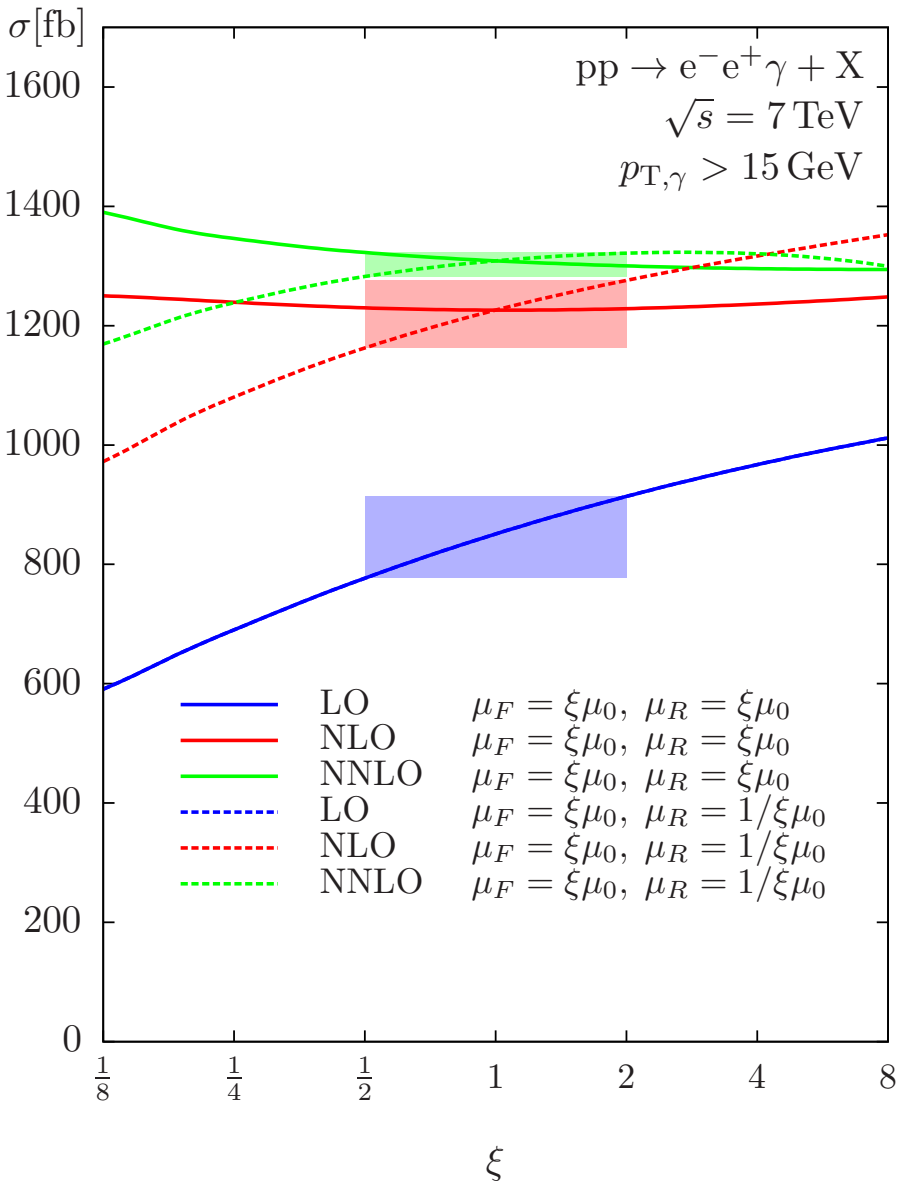

- Scale variation essentially disappears at NLO and NNLO if variation with $\mu_F = \mu_R$ is considered.

  $\hookrightarrow$ accidental cancellation between μ_F and μ_R dependence!

- Solution: antipodal scale variation: $\mu_F = \xi\mu_0,\ \mu_R = 1/\xi\mu_0,\ \xi \in [0.5,2]$ (also proposed by [Campbell, Ellis, Williams (2011)])

Resulting scale variation ($\mu_R,\ \mu_F \in [0.5\mu_0, 2\mu_0]$) :

LO	NLO	NNLO
$^{+7\%}_{-9\%}$	$^{+4\%}_{-5\%}$	$^{+1\%}_{-2\%}$

Scale variation (LHC @ 7 TeV, ATLAS setup, $p_{T,\gamma} > 40\,\mathrm{GeV}$)

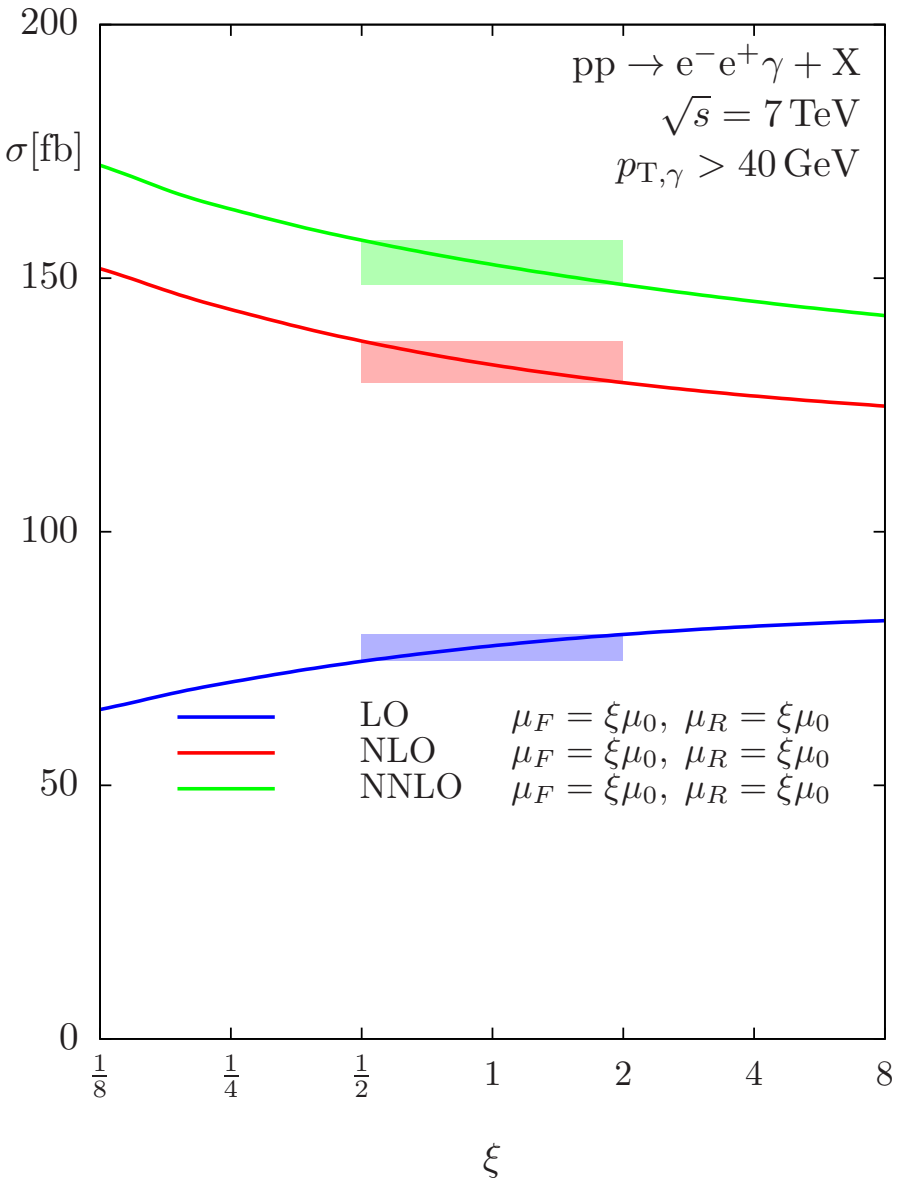

- Due to higher cut on $p_{T,\gamma}$, higher CMS energies (thereby higher x_1, x_2) involved.
  - Cross-section dependence on μ_F decreases (wrt. to lower $p_{T,\gamma}$ cut).
  - No significant cancellation between μ_F and μ_R dependence.
  - μ_R dominates scale dependence.
- Consider independent variations of μ_F and μ_R and take the envelope.

Resulting scale variation ($\mu_R,\ \mu_F \in [0.5\mu_0, 2\mu_0]$) :

LO	NLO	NNLO
$^{+3\%}_{-4\%}$	$^{+4\%}_{-4\%}$	$^{+3\%}_{-3\%}$

Scale variation (LHC @ 7 TeV, ATLAS setup, $p_{T,\gamma} > 40\,\mathrm{GeV}$)

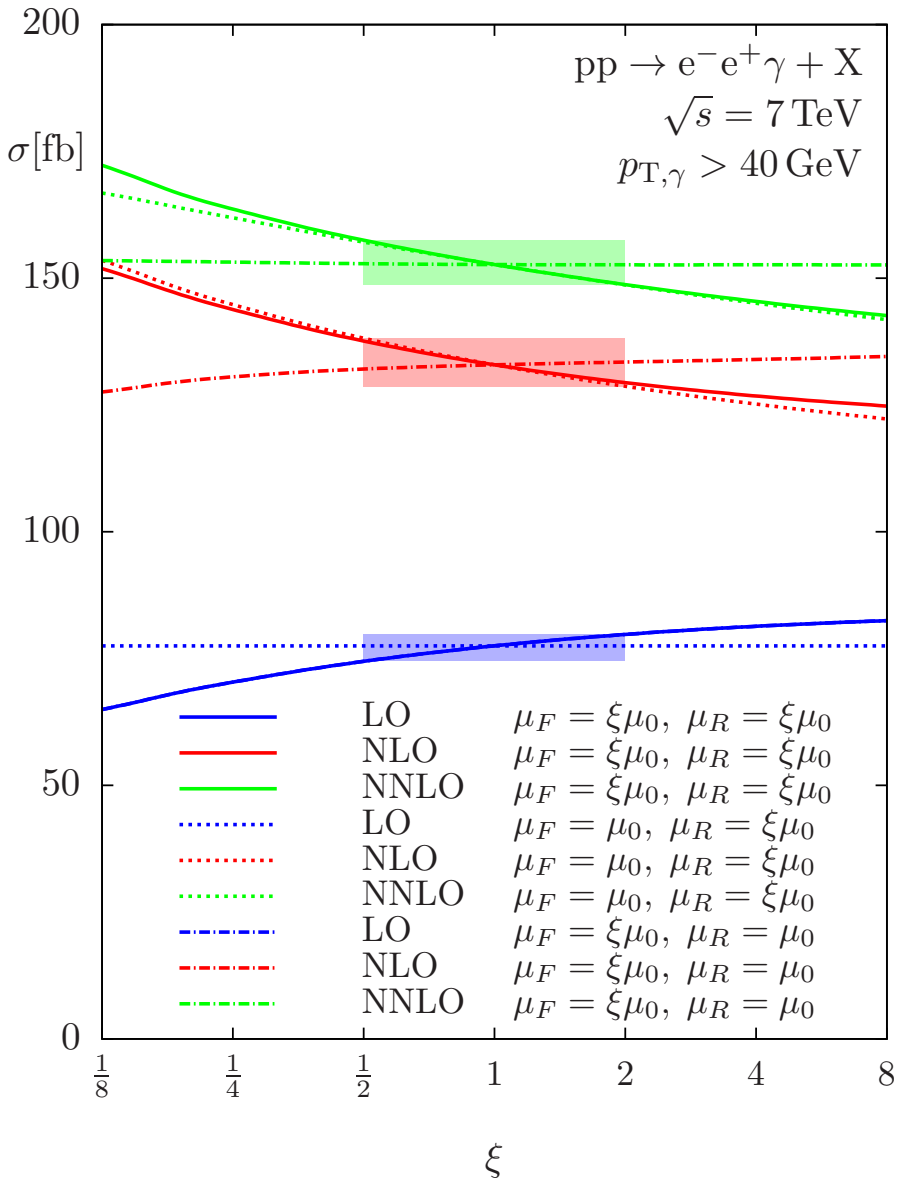

- Due to higher cut on $p_{T,\gamma}$, higher CMS energies (thereby higher x_1, x_2) involved.
  - Cross-section dependence on μ_F decreases (wrt. to lower $p_{T,\gamma}$ cut).
  - No significant cancellation between μ_F and μ_R dependence.
  - μ_R dominates scale dependence.
- Consider independent variations of μ_F and μ_R and take the envelope.

Resulting scale variation ($\mu_R,\ \mu_F \in [0.5\mu_0, 2\mu_0]$) :

LO	NLO	NNLO
$^{+3\%}_{-4\%}$	$^{+4\%}_{-4\%}$	$^{+3\%}_{-3\%}$

Scale variation (LHC @ 7 TeV, ATLAS setup, $p_{T,\gamma} > 40\,\mathrm{GeV}$)

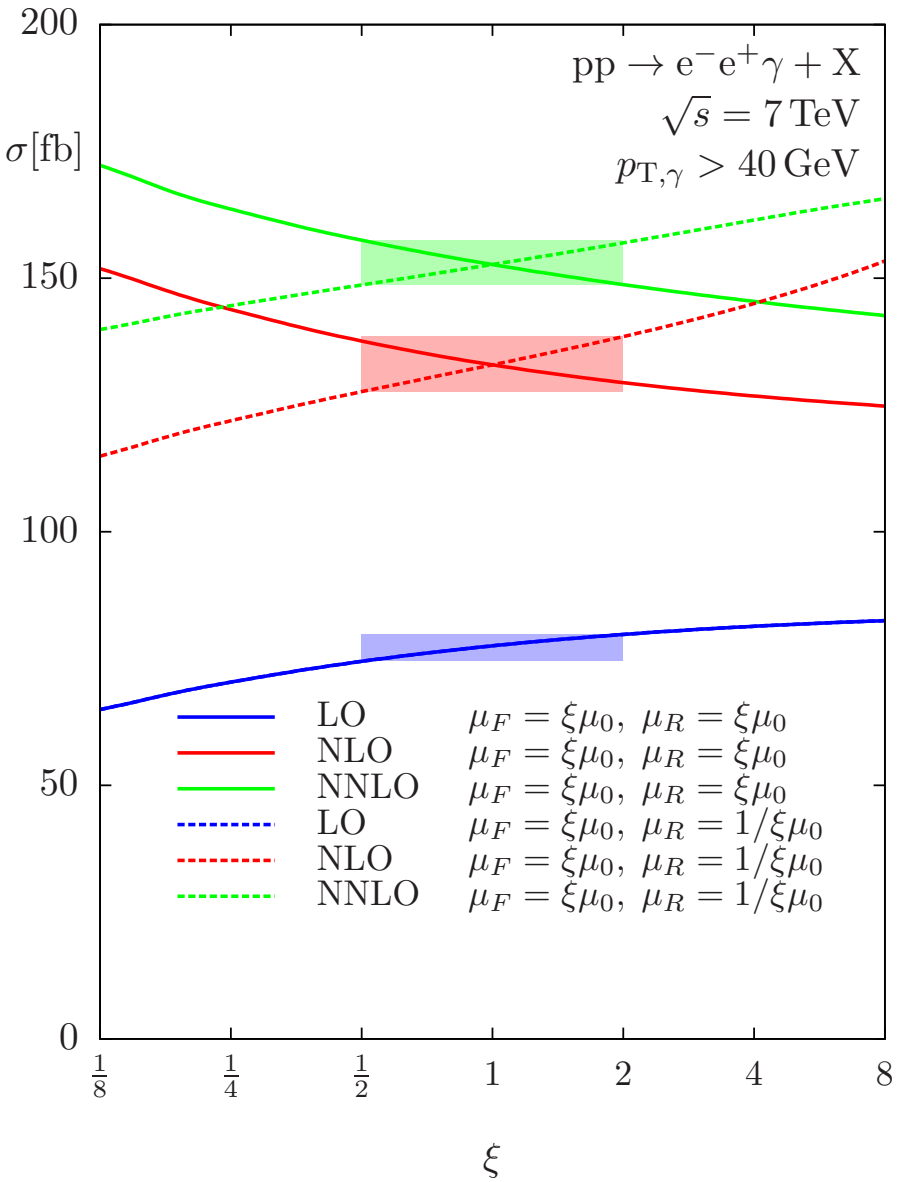

- Due to higher cut on $p_{T,\gamma}$, higher CMS energies (thereby higher x_1, x_2) involved.
  - Cross-section dependence on μ_F decreases (wrt. to lower $p_{T,\gamma}$ cut).
  - No significant cancellation between μ_F and μ_R dependence.
  - μ_R dominates scale dependence.
- Consider independent variations of μ_F and μ_R and take the envelope.

Resulting scale variation ($\mu_R,\ \mu_F \in [0.5\mu_0, 2\mu_0]$) :

LO	NLO	NNLO
$^{+3\%}_{-4\%}$	$^{+4\%}_{-4\%}$	$^{+3\%}_{-3\%}$

Integrated $Z\gamma$ cross-section predictions (LHC @ 7 TeV)

- Integrated cross sections:

	LO	NLO	NNLO	experiment
ATLAS setup $p_T^\gamma > 15\,\mathrm{GeV}$	$0.8507[2]^{+7\%}_{-9\%}$ pb	$1.2262[4]^{+4\%}_{-5\%}$ pb	$1.305[3]^{+1\%}_{-2\%}$ pb	$1.310 \pm .020(\mathrm{stat}) \pm .110(\mathrm{syst}) \pm .050(\mathrm{lumi})$ pb
ATLAS setup $p_T^\gamma > 40\,\mathrm{GeV}$	$77.48[6]^{+3\%}_{-4\%}$ fb	$132.89[7]^{+4\%}_{-4\%}$ fb	$152.5[5]^{+3\%}_{-3\%}$ fb	
CMS setup $p_T^\gamma > 15\,\mathrm{GeV}$	$1.3336[2]^{+8\%}_{-9\%}$ pb	$1.8438[7]^{+4\%}_{-5\%}$ pb	$1.917[8]^{+2\%}_{-3\%}$ pb	

- Relative (compared to previous order) size of corrections:

		NLO/LO	NNLO/NLO
ATLAS setup	$p_T^\gamma > 15\,\mathrm{GeV}$	+44%	+6%
ATLAS setup	$p_T^\gamma > 40\,\mathrm{GeV}$	+72%	+15%
CMS setup	$p_T^\gamma > 15\,\mathrm{GeV}$	+38%	+4%

- Loop-induced gg contribution turns out to be very small ($< 10\%$ of NNLO).

Data comparison: p_T^γ (LHC @ 7 TeV, ATLAS setup, $p_{T,\gamma} > 15\,\mathrm{GeV}$)

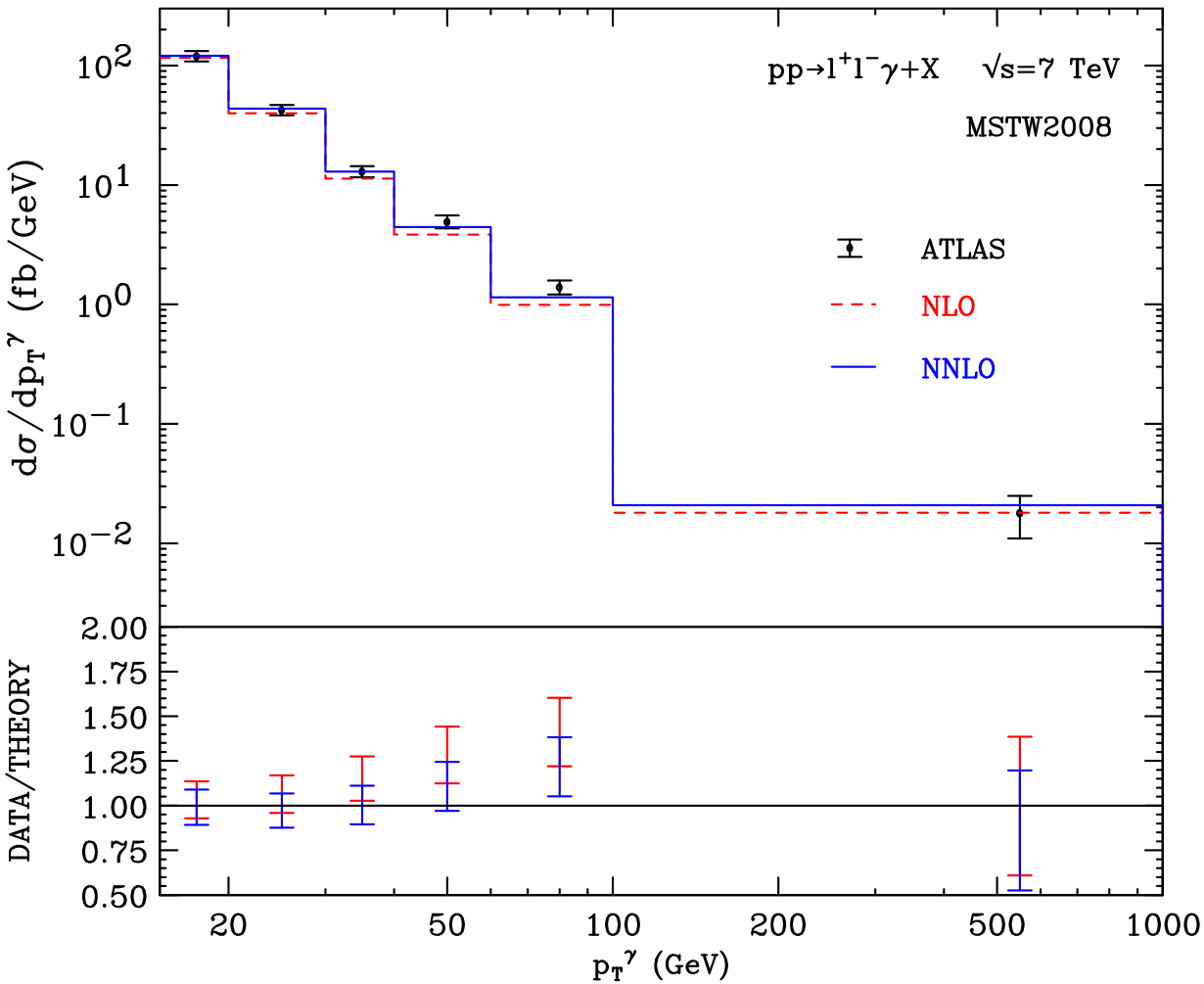

- Similarly good agreement between data and theory at both NLO and NNLO.
- No electroweak corrections included (possibly large effects in high-p_T region).

Distribution in $M_{l^-l^+}$ (LHC @ 7 TeV, ATLAS setup, $p_{T,\gamma} > 15\,\text{GeV}$)

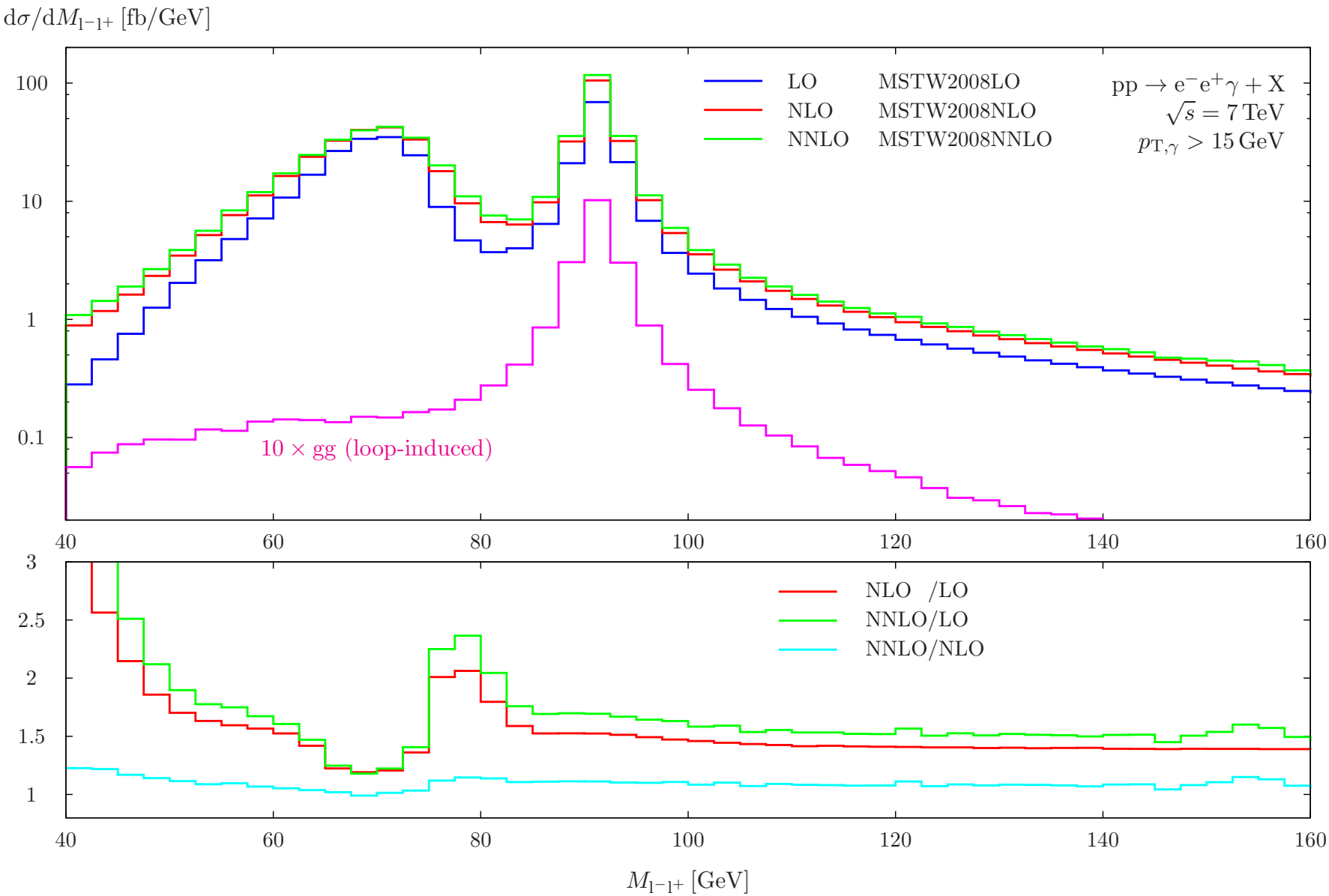

Distribution in $M_{l^-l^+\gamma}$ (LHC @ 7 TeV, ATLAS setup, $p_{T,\gamma} > 15\,\text{GeV}$)

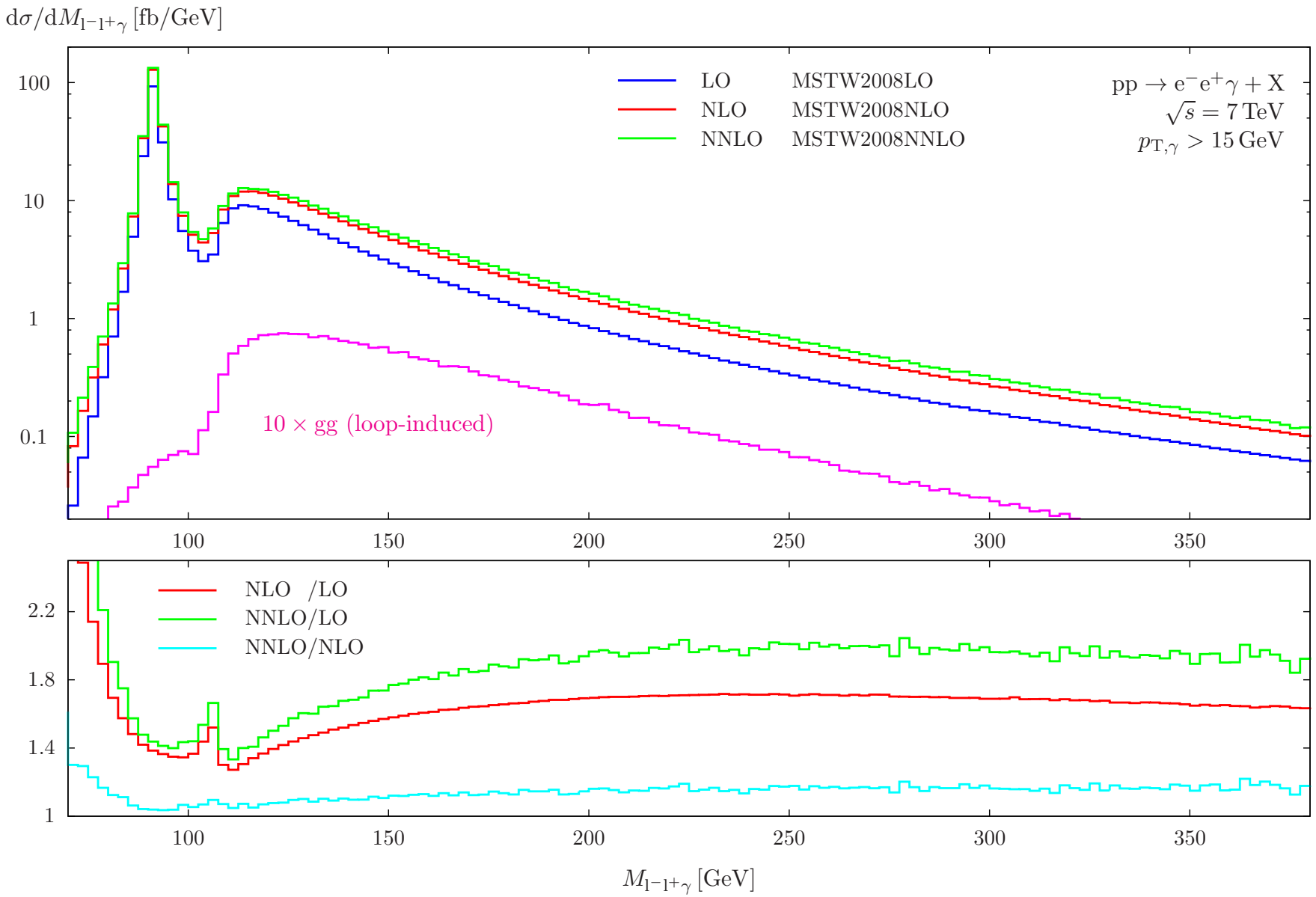

Distribution in $M_{l^-l^+\gamma}$ (LHC @ 7 TeV, ATLAS setup, $p_{T,\gamma} > 40\,\text{GeV}$)

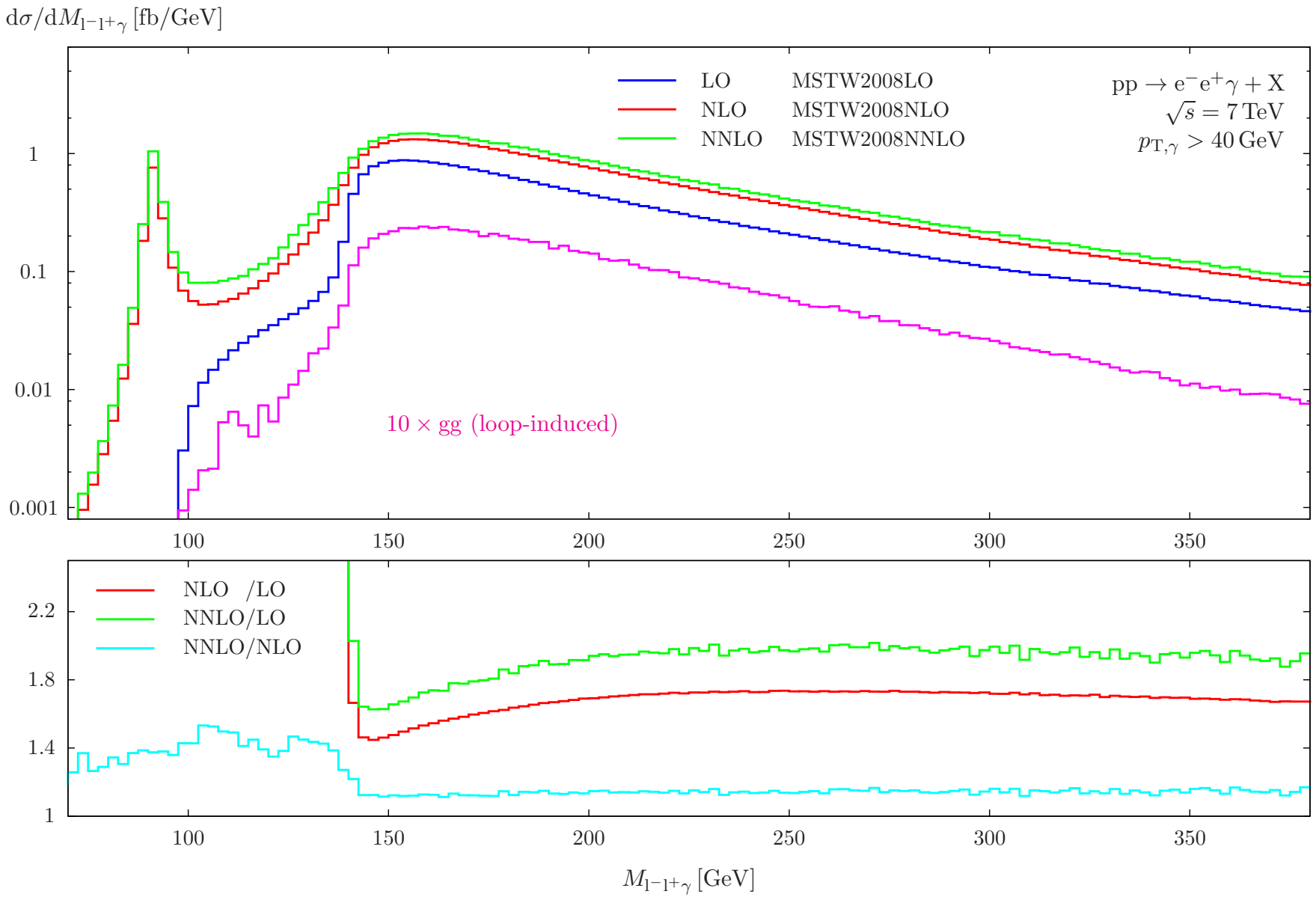

Numerical results for $\mathrm{pp} \to \mathrm{W}^{\pm}\gamma + \mathrm{X}$ at NNLO QCD

Integrated $W^{\pm}\gamma$ cross-section predictions (LHC @ 7 TeV)

- Integrated cross sections (ATLAS setup [arXiv:1302.1283]):
  - close to ATLAS $Z\gamma$ setup with $p_T^{\gamma} > 15\,\mathrm{GeV}$,
  - only adaptation: $m_{l^-l^+} > 40\,\mathrm{GeV}$ replaced by $p_{\mathrm{miss,T}} > 35\,\mathrm{GeV}$.

	LO	NLO	NNLO	experiment
$W^+\gamma$	$0.51112[6]^{+6\%}_{-7\%}$ pb	$1.1545[2]^{+5\%}_{-4\%}$ pb	$1.361[6]^{+4\%}_{-3\%}$ pb	
$W^-\gamma$	$0.39531[4]^{+6\%}_{-8\%}$ pb	$0.9106[2]^{+5\%}_{-4\%}$ pb	$1.074[6]^{+3\%}_{-3\%}$ pb	
$W^{\pm}\gamma$	$0.90642[7]^{+6\%}_{-8\%}$ pb	$2.0651[3]^{+5\%}_{-4\%}$ pb	$2.435[8]^{+4\%}_{-3\%}$ pb	$2.770\ {}^{\pm.030\,(\mathrm{stat})}_{\pm.330\,(\mathrm{stat})}{}^{\pm.140\,(\mathrm{lumi})}$ pb

$\hookrightarrow \sim 2\sigma$ tension between data and NLO result is cured by NNLO correction!

- Relative (compared to previous order) size of corrections:

	NLO/LO	NNLO/NLO
$W^+\gamma$	+126%	+18%
$W^-\gamma$	+130%	+18%

- Breaking of "radiation zero" could explain large corrections.

Data comparison: p_T^{γ} (LHC @ 7 TeV, ATLAS setup, $p_{T,\gamma} > 15\,\mathrm{GeV}$)

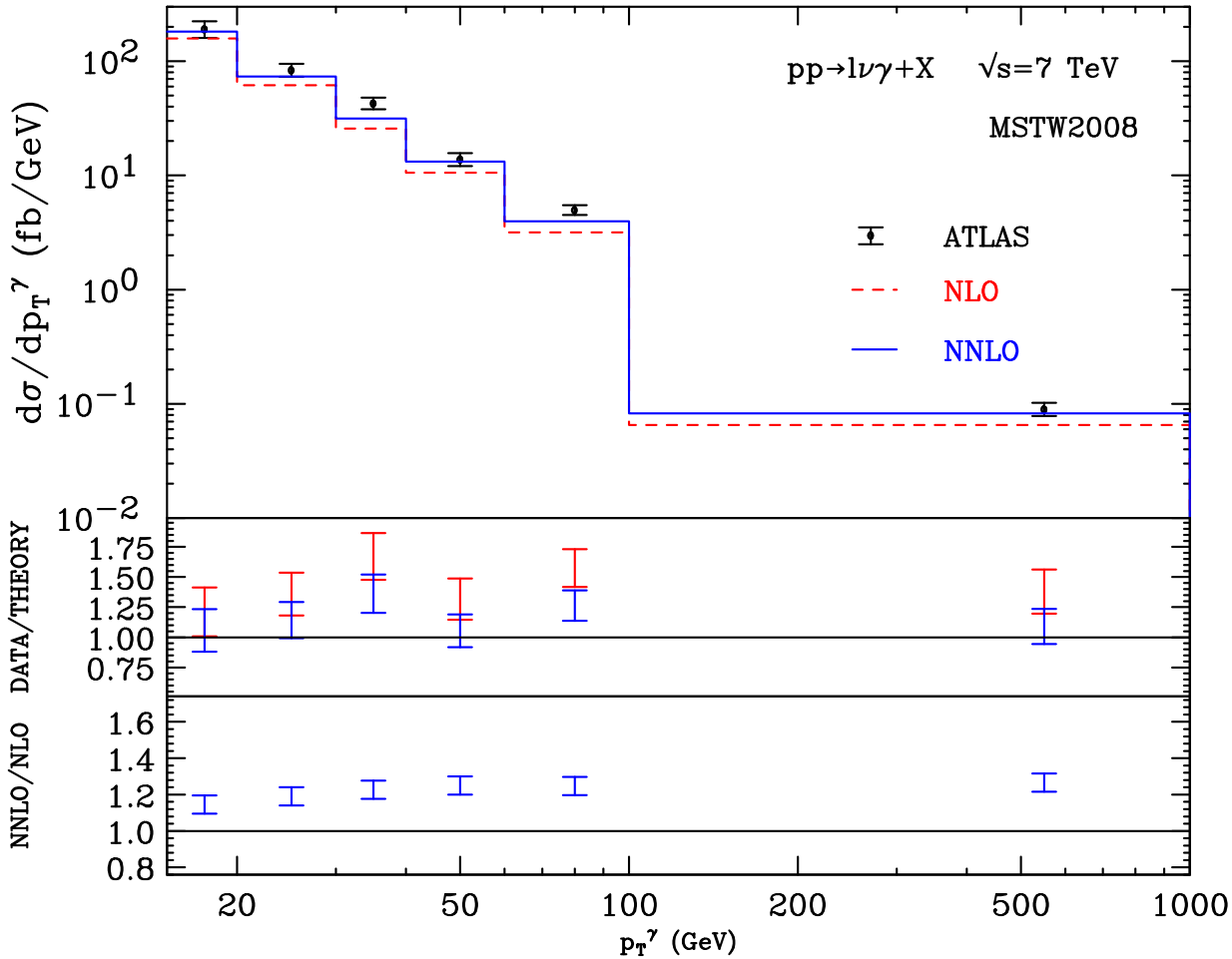

- Agreement between data and theory significantly improved by NNLO corrections.
- No electroweak corrections included (possibly large effects in high-p_T region).

Numerical results for $\mathrm{pp} \to \mathrm{ZZ} + \mathrm{X}$ at NNLO QCD

Inclusive ZZ cross sections for relevant LHC energies

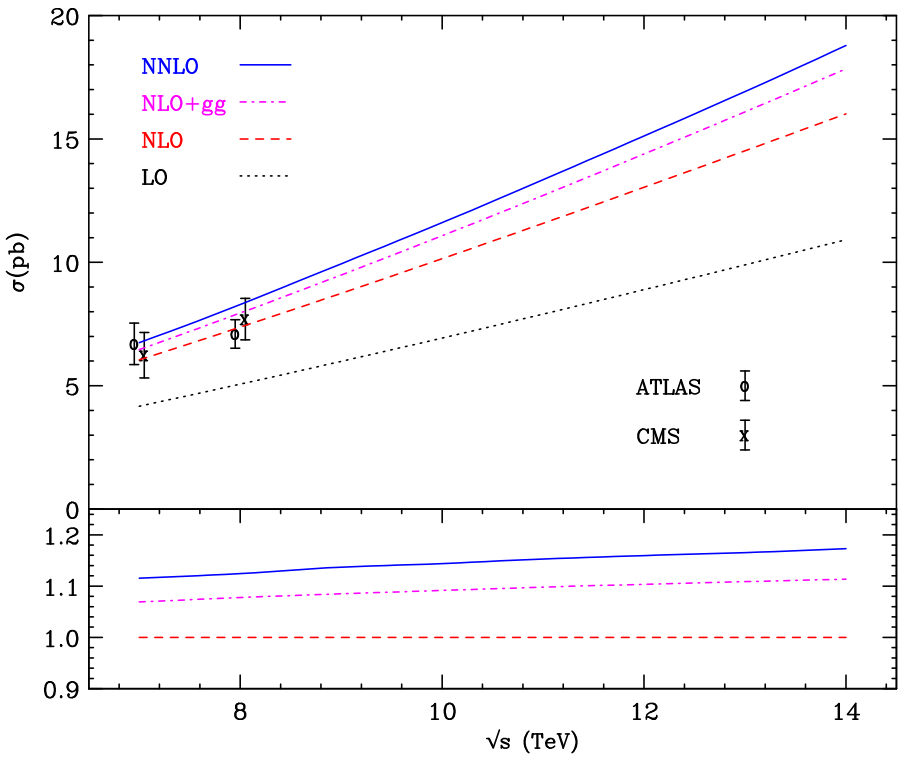

$\sqrt{s}$ [TeV]	σ_{LO} [pb]	σ_{NLO} [pb]	σ_{NNLO} [pb]
7	$4.172^{+0.7\%}_{-1.6\%}$	$6.049^{+2.8\%}_{-2.2\%}$	$6.747^{+2.9\%}_{-2.3\%}$
8	$5.066^{+2.7\%}_{-1.6\%}$	$7.376^{+2.8\%}_{-2.3\%}$	$8.294^{+3.0\%}_{-2.3\%}$
9	$5.988^{+2.4\%}_{-3.5\%}$	$8.744^{+2.9\%}_{-2.3\%}$	$9.964^{+3.2\%}_{-2.5\%}$
10	$6.935^{+3.1\%}_{-4.3\%}$	$10.15^{+2.9\%}_{-2.3\%}$	$11.63^{+3.3\%}_{-2.5\%}$
11	$7.904^{+3.8\%}_{-5.0\%}$	$11.58^{+3.0\%}_{-2.4\%}$	$13.33^{+3.3\%}_{-2.4\%}$
12	$8.893^{+4.3\%}_{-5.6\%}$	$13.04^{+3.0\%}_{-2.4\%}$	$15.13^{+3.2\%}_{-2.5\%}$
13	$9.899^{+4.9\%}_{-6.1\%}$	$14.52^{+3.0\%}_{-2.4\%}$	$16.93^{+3.3\%}_{-2.4\%}$
14	$10.92^{+5.4\%}_{-6.7\%}$	$16.02^{+3.0\%}_{-2.4\%}$	$18.80^{+3.3\%}_{-2.4\%}$

- Scale uncertainties ($M_{\mathrm{Z}}/2 < \mu_{\mathrm{R}}, \mu_{\mathrm{F}} < 2M_{\mathrm{Z}}$, $1/2 < \mu_{\mathrm{R}}/\mu_{\mathrm{F}} < 2$) remain about $\pm 3\%$.
- LO, NLO, and NNLO bands don't overlap $\rightarrow$ underestimation of missing higher orders.
- Loop-induced gg channel provides about 60% of NNLO effect.
- NNLO/NLO ranges from 12% to 17% when $\sqrt{s}$ varies from 7 TeV to 14 TeV.
- No electroweak corrections included.

Numerical results for $\mathrm{pp} \to \mathrm{W^+W^-} + \mathrm{X}$ at NNLO QCD

Definition of top-contamination free WW cross section in 5FNS

Definition of WW cross section beyond LO

- straightforward in 4FNS (massive b's)
- non-trivial in 5FNS (massless b's)
  - Single-top production enters at NLO.

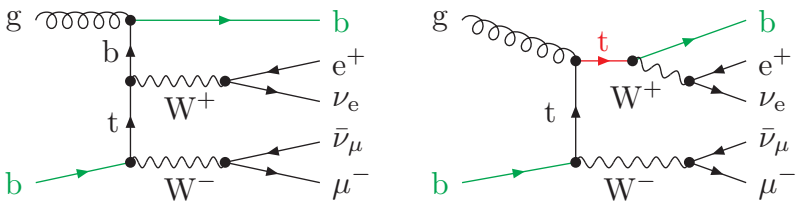

  - Top-pair production enters at NNLO.

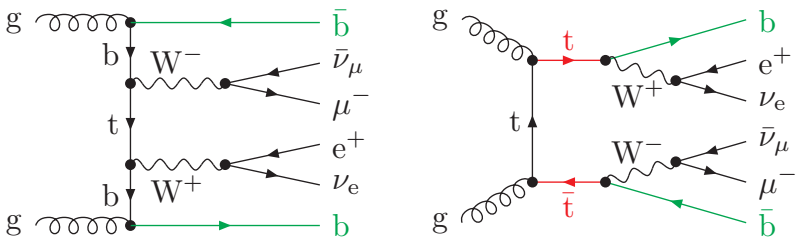

↪ Huge "higher-order corrections" from top-resonance contamination in 5FNS.

Definition of top-contamination free WW cross section in 5FNS

Definition of WW cross section beyond LO

- straightforward in 4FNS (massive b's)
- non-trivial in 5FNS (massless b's)
  - Single-top production enters at NLO.

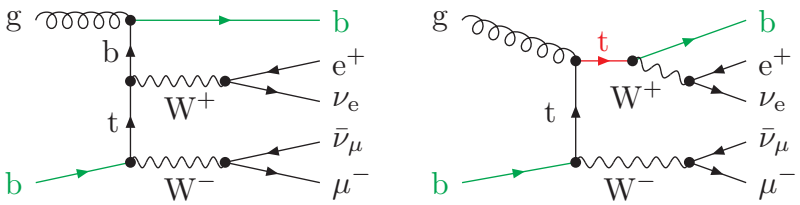

  - Top-pair production enters at NNLO.

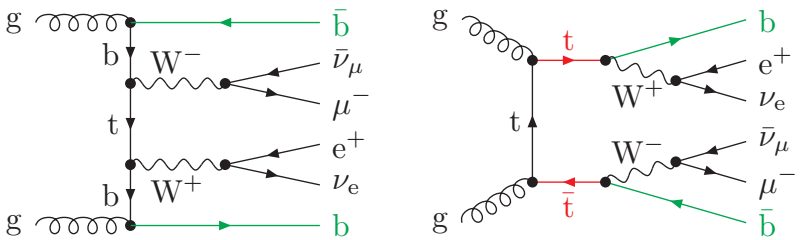

↪ Huge "higher-order corrections" from top-resonance contamination in 5FNS.

Γ_t-dependence of NNLO cross section can be used to isolate the different processes:

$$\sigma_{WW} \propto 1, \quad \sigma_{tW} \propto 1/\Gamma_t, \quad \sigma_{t\bar{t}} \propto 1/\Gamma_t^2.$$

↪ Parabolic fit of the $(\Gamma_t/\Gamma_t^{\text{phys}})^2$-rescaled cross section delivers σ_{WW}, σ_{tW}, $\sigma_{t\bar{t}}$.

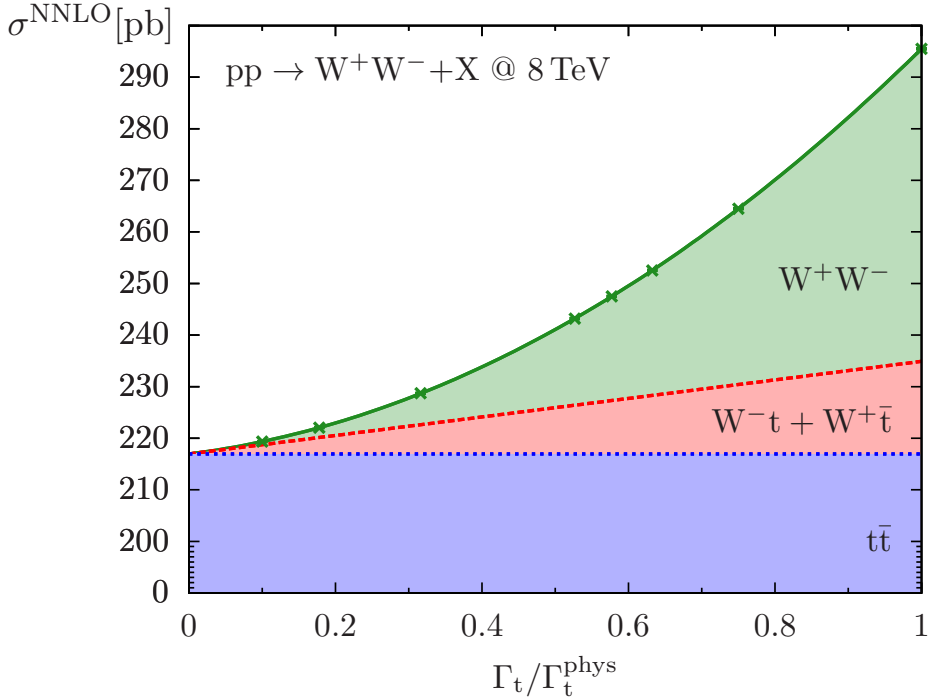

Comparison between 4FNS and 5FNS WW cross sections

- Cross-section enhancement of 30%/400% at NLO/NNLO due to top contamination.
- About 15% of enhancement remain at NNLO for "physical" $p_{T,bjet}^{veto} \approx 30\,GeV$.
- The limit $p_{T,bjet}^{veto} \to 0\,GeV$ cannot be directly accessed (Infrared divergent in 5FNS).

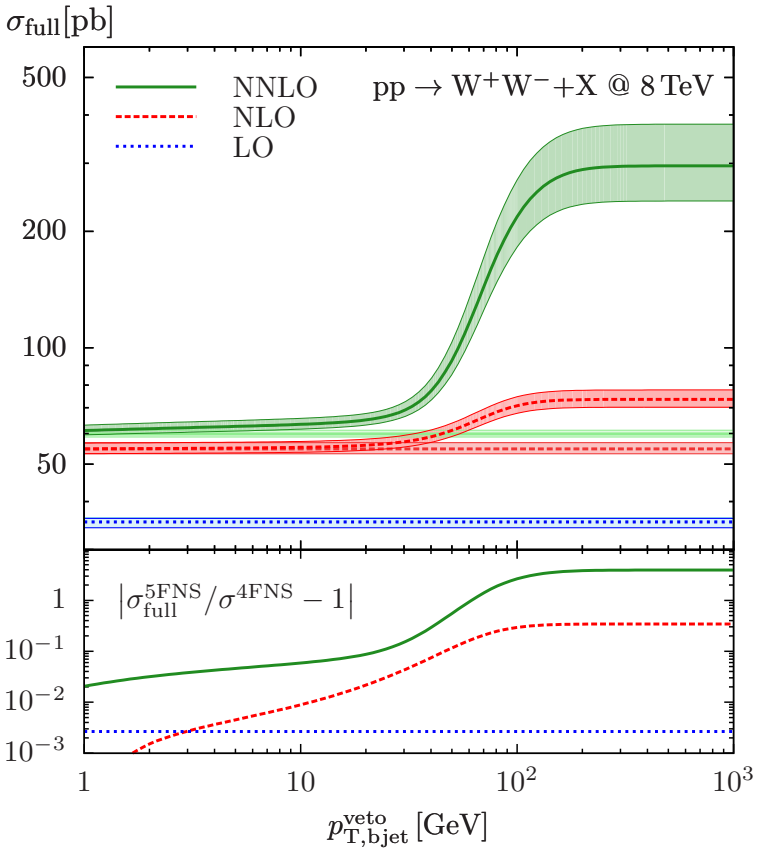

Comparison between 4FNS and 5FNS WW cross sections

- Cross-section enhancement of 30%/400% at NLO/NNLO due to top contamination.
- About 15% of enhancement remain at NNLO for "physical" $p_{T,bjet}^{veto} \approx 30\,GeV$.
- The limit $p_{T,bjet}^{veto} \to 0\,GeV$ cannot be directly accessed (Infrared divergent in 5FNS).

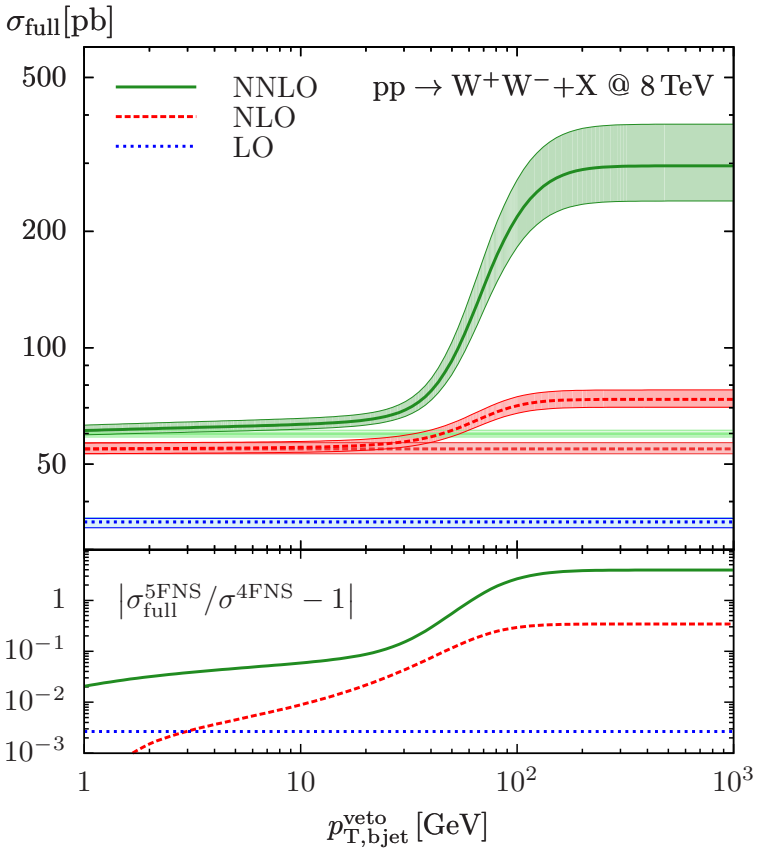

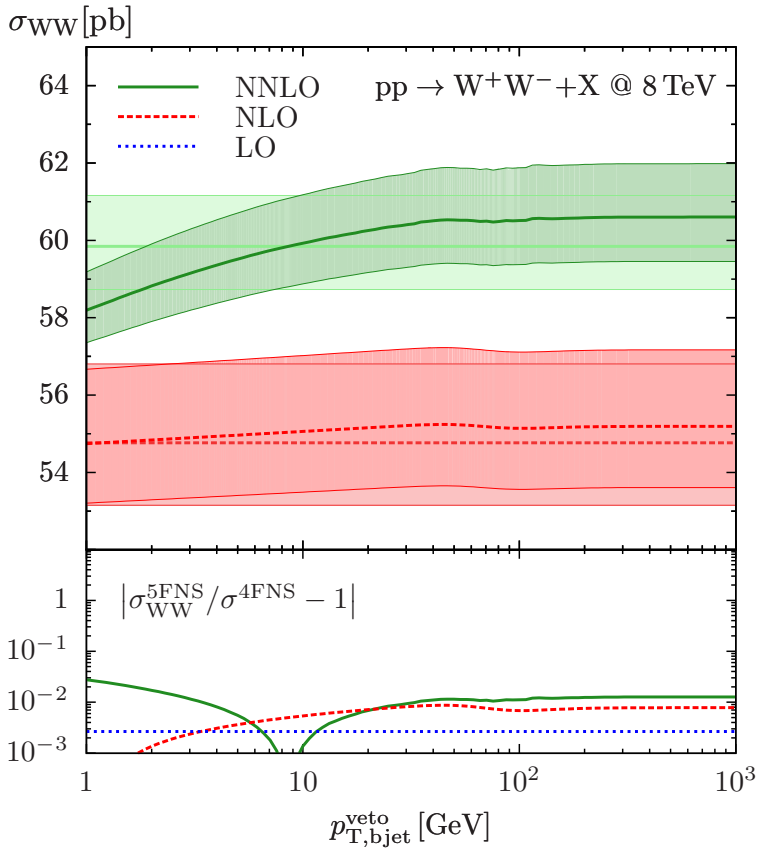

↪ Extrapolation gives ≈ 1-2% agreement between 4FNS and 5FNS for $p_{T,bjet}^{veto} \to \infty$.

Inclusive WW cross sections in 4FNS for relevant LHC energies

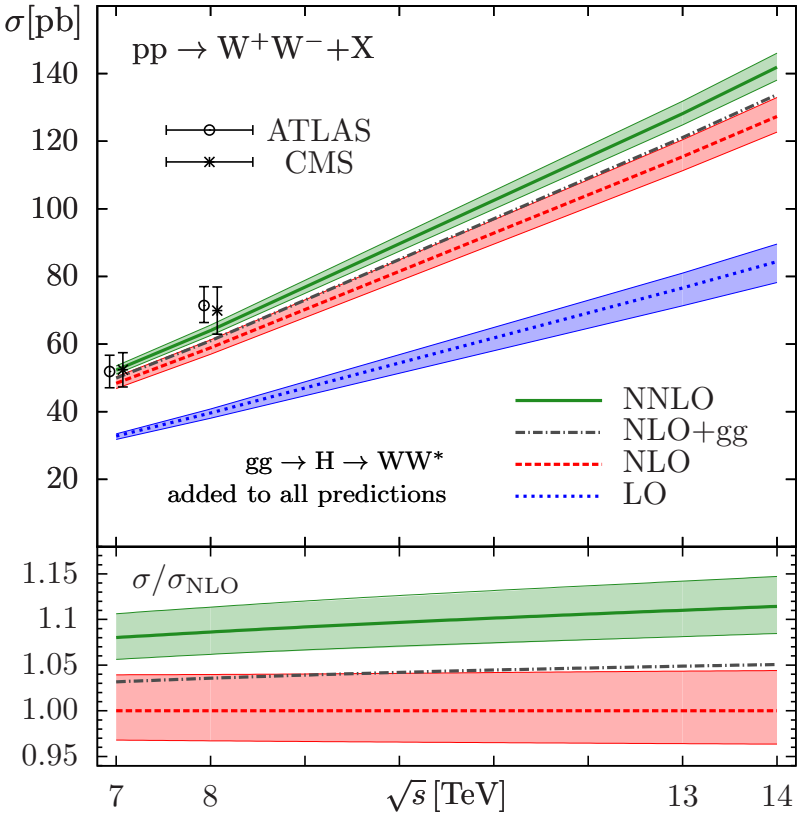

$\sqrt{s}$ [TeV]	σ_{LO} [pb]	σ_{NLO} [pb]	σ_{NNLO} [pb]	$\sigma_{\mathrm{gg\to H\to WW^*}}$ [pb]
7	$29.52^{+1.6\%}_{-2.5\%}$	$45.16^{+3.7\%}_{-2.9\%}$	$49.04^{+2.1\%}_{-1.8\%}$	$3.25^{+7.1\%}_{-7.8\%}$
8	$35.50^{+2.4\%}_{-3.5\%}$	$54.77^{+3.7\%}_{-2.9\%}$	$59.84^{+2.2\%}_{-1.9\%}$	$4.14^{+7.2\%}_{-7.8\%}$
13	$67.16^{+5.5\%}_{-6.7\%}$	$106.0^{+4.1\%}_{-3.2\%}$	$118.7^{+2.5\%}_{-2.2\%}$	$9.44^{+7.4\%}_{-7.9\%}$
14	$73.74^{+5.9\%}_{-7.2\%}$	$116.7^{+4.1\%}_{-3.3\%}$	$131.3^{+2.6\%}_{-2.2\%}$	$10.64^{+7.5\%}_{-8.0\%}$

- Scale-variation uncertainties are about $\pm 3\%$ ($M_{\mathrm{W}}/2 < \mu_{\mathrm{R}}, \mu_{\mathrm{F}} < 2M_{\mathrm{W}}$, $1/2 < \mu_{\mathrm{R}}/\mu_{\mathrm{F}} < 2$).
- Loop-induced gg channel provides about 35% of NNLO effect.
- NNLO/NLO ranges from 9% to 12% when $\sqrt{s}$ varies from 7 TeV to 14 TeV.

- 2σ excess in ATLAS 8TeV data is clearly reduced by positive NNLO corrections.
- Further corrections should be taken into account: • off-shell effects • EW corrections • photon-induced contributions • NLO QCD for loop-induced gg channel • ...
- Calculation of fiducial cross sections could circumvent possible extrapolation problems.

Conclusions & Outlook

Conclusions

- Widely automated framework to perform fully differential NNLO QCD computations for the production of colourless final states, based on q_{T} subtraction.
- Fully differential NNLO QCD results for $\mathrm{pp} \to \mathrm{V}\gamma + \mathrm{X}$ presented.
  - Full leptonic decays with spin correlations and off-shell effects included.
  - NNLO corrections for $\mathrm{W}^{\pm}\gamma$ larger than for $\mathrm{Z}\gamma$ (radiation zero).
  - Loop-induced gg contribution turns out to be very small ($< 10\%$ of NNLO).
    $\hookrightarrow$ clearly does not cover the main part of the NNLO corrections.
- Inclusive NNLO QCD results for $\mathrm{pp} \to \mathrm{ZZ}/\mathrm{W}^{+}\mathrm{W}^{-} + \mathrm{X}$ presented.
  - Sizable NNLO corrections of about 15%/10% (with respect to NLO).
  - Loop-induced gg-channel contributes about 60%/35% of the NNLO corrections.

Outlook

- More phenomenological studies on $\mathrm{pp} \to \mathrm{V}\gamma + \mathrm{X}$, in particular for $\mathrm{W}\gamma$.
- Extension to helicity amplitudes with two different masses facilitates the differential calculation of off-shell $\mathrm{W}^{+}\mathrm{W}^{-}$, $\mathrm{W}^{\pm}\mathrm{Z}$ and ZZ production with full leptonic decays.
  $\hookrightarrow$ Fiducial cross sections can be directly calculated at NNLO accuracy soon!

Backup

Backup slides

Status of $pp \to VV'$+X towards NNLO QCD

Four levels of complexity (essentially in terms of 2-loop amplitudes):

- $\mathbf{pp \to \gamma\gamma + X}$ (two massless vector bosons)
  - $\mathrm{pp} \to \gamma\gamma + \mathrm{jet} + \mathrm{X}$ at NLO QCD known.
    [Del Duca, Maltoni, Nagy, Trocsanyi (2003)]
  - Loop-induced gg-channel known.
    [Dicus, Willenbrock (1988)]; [Li, Xiangdong (2013)]
  - 2-loop amplitudes known.
    [Anastasiou, Glover, Tejeda–Yeomans (2002)]
  - NNLO QCD calculation of $\mathrm{pp} \to \gamma\gamma + \mathrm{X}$ completed via q_T subtraction.
    [Catani, Cieri, de Florian, Ferrera, Grazzini (2011)]

- $\mathbf{pp \to V\gamma + X}$ (one massless, one massive vector boson)
  - $\mathrm{pp} \to \mathrm{V}\gamma + \mathrm{jet} + \mathrm{X}$ at NLO QCD known.
    [Campanario, Englert, Spannowsky (2009)]; [Campbell, Hartanto, Williams (2012)]
  - Loop-induced gg-channel known.
    [Amettler, Gava, Paver, Treleani (1985)]; [van der Bij, Glover (1988)];
    [Adamson, de Florian, Signer (2003)]; [Gehrmann, Tancredi, Weihs (2013)]
  - 2-loop amplitudes known both for $\mathrm{Z}\gamma$ and for $\mathrm{W}^\pm\gamma$.
    [Gehrmann, Tancredi (2012)]; [Matsuura, van der Marck, van Neerven (1989)]
  - NNLO QCD calculation of $\mathrm{pp} \to \mathrm{Z}\gamma/\mathrm{W}^\pm\gamma + \mathrm{X}$ (with decays) completed.
    [Grazzini, SK, Rathlev, Torre ($\mathrm{Z}\gamma$: 2013, $\mathrm{W}\gamma$: to be published...)]

Status of $pp \to VV'$+X towards NNLO QCD

- $\mathbf{pp \to VV' + X}$ (two massive vector bosons with $m_{\mathrm{V}} = m_{\mathrm{V}'}$ (on shell V/V'))
  - $\mathrm{pp} \to \mathrm{W^+W^-/ZZ} + \mathrm{jet} + \mathrm{X}$ at NLO QCD known.
    [Dittmaier, SK, Uwer (2007)]; [Campbell, Ellis, Zanderighi (2007)]; [Binoth, Gleisberg, Karg, Kauer, Sanguinetti (2009)]
  - Loop-induced gg-channel known.
    [van der Bij, Glover (1988)]
  - Master integrals for (planar and non-planar) 2-loop topologies known.
    [Gehrmann, von Manteuffel, Tancredi, Weihs (2013 & 2014)]
  - 2-loop WW amplitudes in high-energy limit (+ mass-dependence reconstruction)
    [Chachamis, Czakon, Eiras (2008)]
  - NNLO QCD calculation of $\mathrm{pp} \to \mathrm{ZZ//W^+W^-} + \mathrm{X}$ (inclusive production) done for stable Z/W bosons via q_{T} subtraction.
    [ZZ: Cascioli, Gehrmann, Grazzini, SK, Maierhöfer, von Manteuffel, Pozzorini, Rathlev, Tancredi, Weihs (2014)]
    [WW: Gehrmann, Grazzini, SK, Maierhöfer, von Manteuffel, Pozzorini, Rathlev, Tancredi (2014)]

- $\mathbf{pp \to VV' + X}$ (two massive vector bosons with $m_{\mathrm{V}} \neq m_{\mathrm{V}'}$)
  - $\mathrm{pp} \to \mathrm{W^\pm Z}(\to \mu^\pm \overset{(-)}{\nu}_\mu \mathrm{e^-e^+}) + \mathrm{jet} + \mathrm{X}$ at NLO QCD known (fully off-shell).
    [Campanario, Englert, SK, Spannowsky, Zeppenfeld (2010)]
  - $\mathrm{pp} \to \mathrm{W^+W^-}(\to \mu^+ \nu_\mu \mathrm{e^-} \bar{\nu}_\mathrm{e}) + \mathrm{jet} + \mathrm{X}$ at NLO QCD known (fully off-shell).
    [Cascioli, Höche, Krauss, Maierhöfer, Pozzorini, Siegert (2014)]
  - Loop-induced gg-channel known.
    [Campbell, Ellis, Williams (2013)]
  - Helicity amplitudes and master integrals known — at least theoretically.
    [Henn, Melnikov, Smirnov (2014)]; [Caola, Henn, Melnikov, Smirnov (2014)]; [Caola, Henn, Melnikov, Smirnov, Smirnov (2014)]

LO Feynman diagrams for $pp \to (V\gamma \to) l\bar{l}'\gamma$

$$pp \to Z\gamma + X \qquad pp \to W\gamma + X$$

$$pp \to \nu_l\bar{\nu}_l\gamma + X \quad pp \to l^-l^+\gamma + X \qquad pp \to l^-\bar{\nu}_l\gamma + X \quad pp \to l^+\nu_l\gamma + X$$

- Photon emission from initial state (anti-)quarks

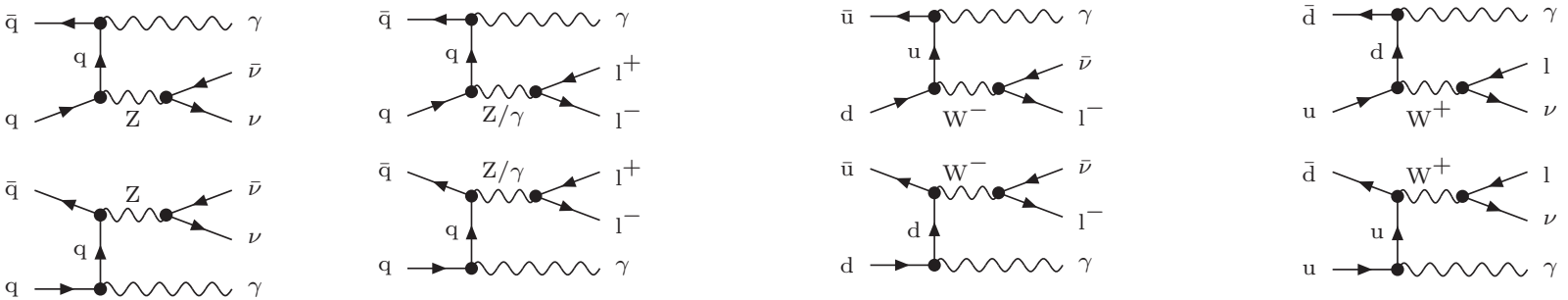

- Photon emission from charged final-state leptons

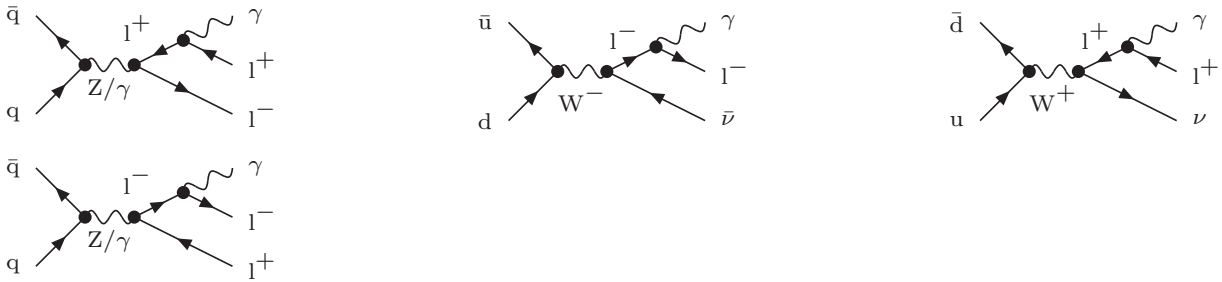

- Photon emission from charged intermediate vector boson

Photon isolation (needed beyond LO)

Two contributions to photon production:

- Direct production in the hard process,
- Non-perturbative fragmentation of a hard parton.

Different approaches to define isolated photons:

- Naive ansatz: forbid any partons inside a fixed cone around the photon.
  ↪ Not infrared safe beyond LO QCD as soft gluons inside the cone are forbidden.
- Hard cone isolation (experimentally preferred):

$$\sum_{\delta' < \delta_0} E_{\mathrm{had,T}}(\delta') \quad \leq \quad \varepsilon_\gamma E_{\gamma,\mathrm{T}}, \qquad\qquad \delta_{i\gamma} = \sqrt{(\eta_i - \eta_\gamma)^2 + (\phi_i - \phi_\gamma)^2}$$

  ↪ Only infrared safe if combined with fragmentation contribution
  (due to quark–photon collinear singularity).
- Smooth cone isolation [Frixione (1998)]:

$$\sum_{\delta' < \delta} E_{\mathrm{had,T}}(\delta') \quad \leq \quad \varepsilon_\gamma E_{\gamma,\mathrm{T}} \left(\frac{1 - \cos(\delta)}{1 - \cos(\delta_0)} \right)^n \quad \forall \quad \delta \leq \delta_0$$

  ↪ Smooth cone isolation eliminates fragmentation contribution completely.

Dependence on q_T (LHC @ 7 TeV, ATLAS setup, $p_{T,\gamma} > 15\,\mathrm{GeV}$)

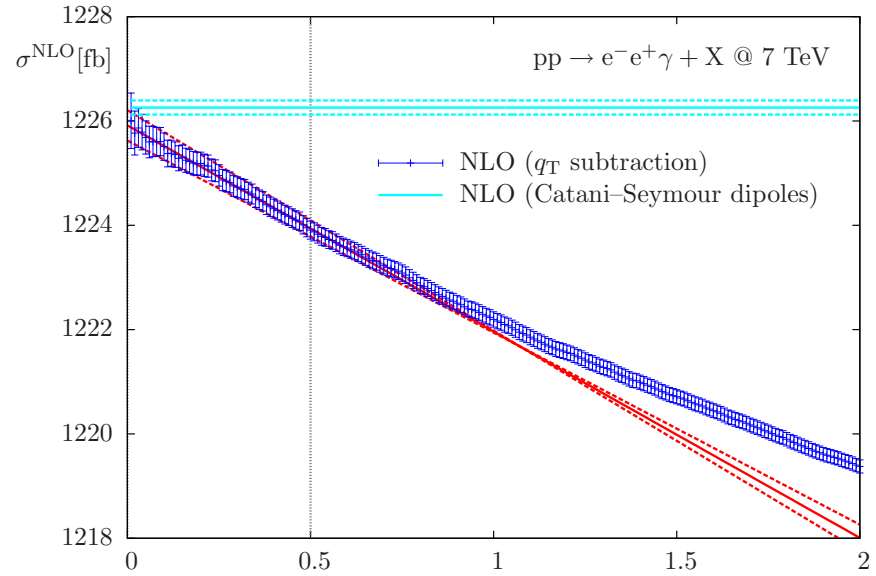

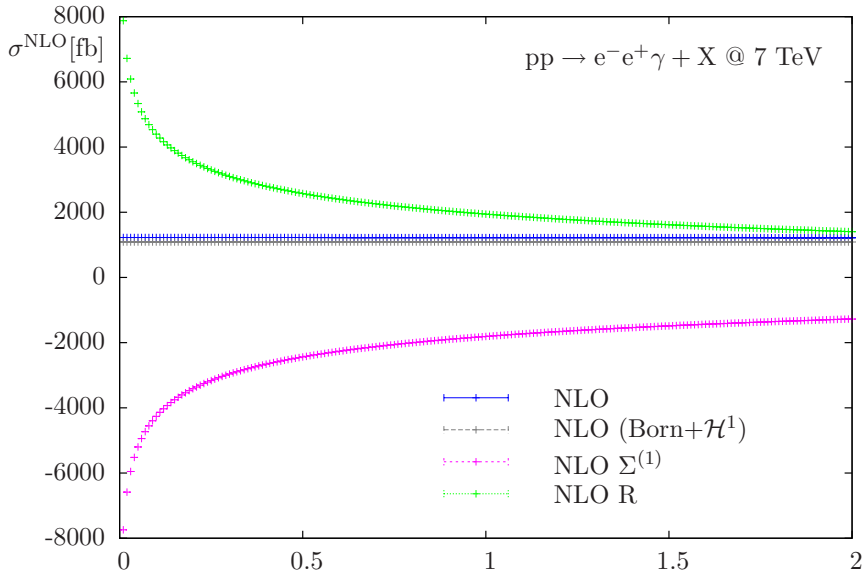

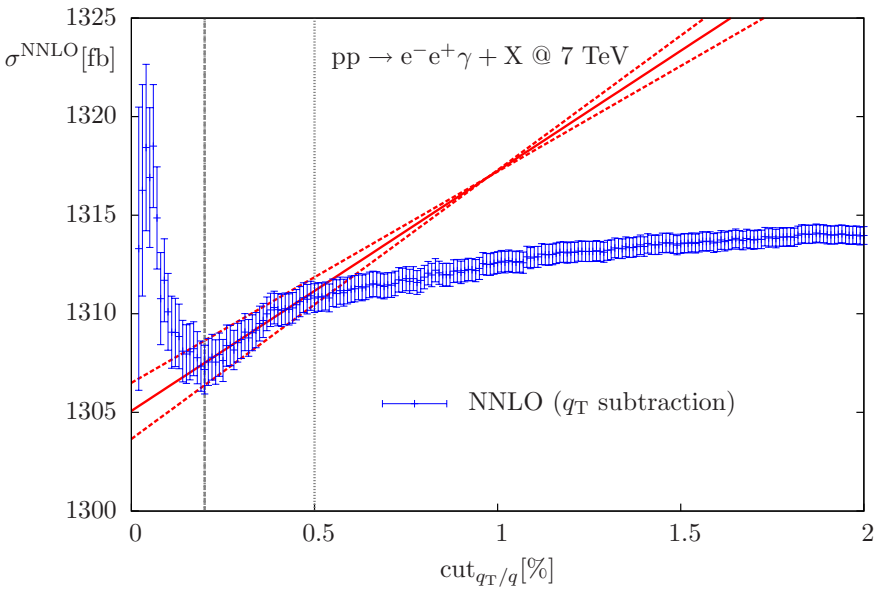

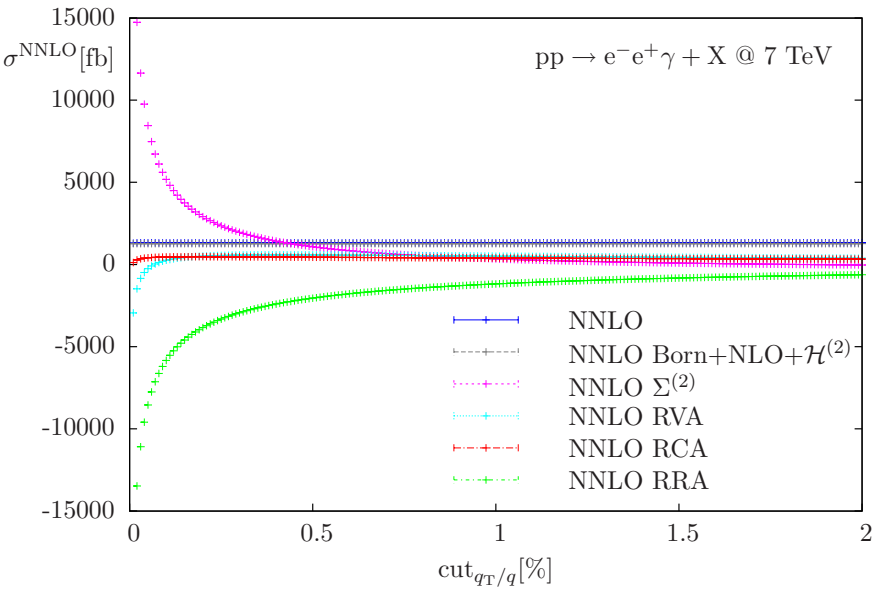

Dependence on q_{T} (LHC @ 8 TeV, LHCb setup, $p_{\mathrm{T},\gamma} > 2\,\mathrm{GeV}$)

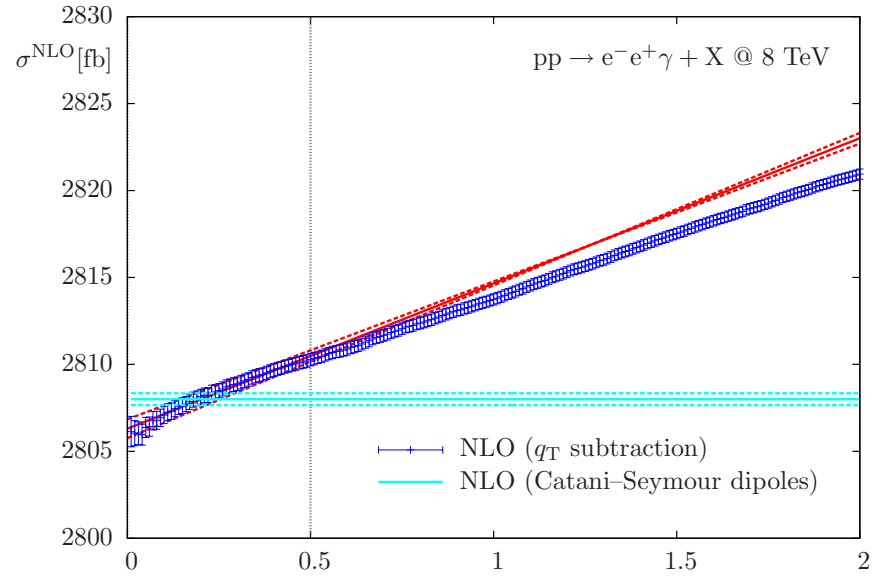

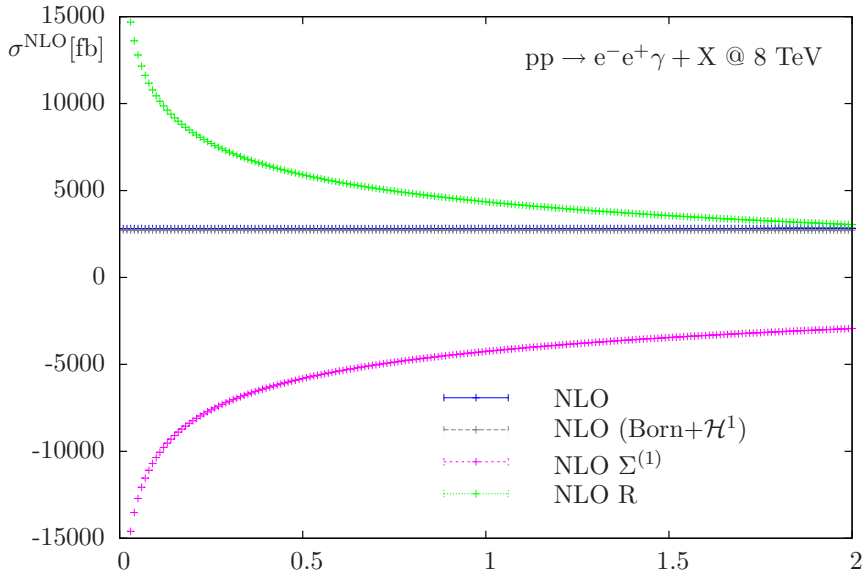

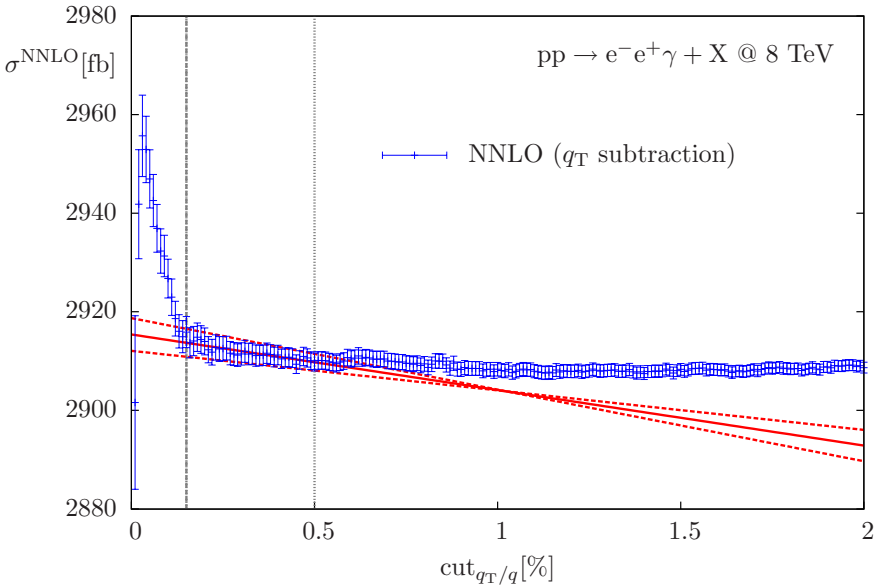

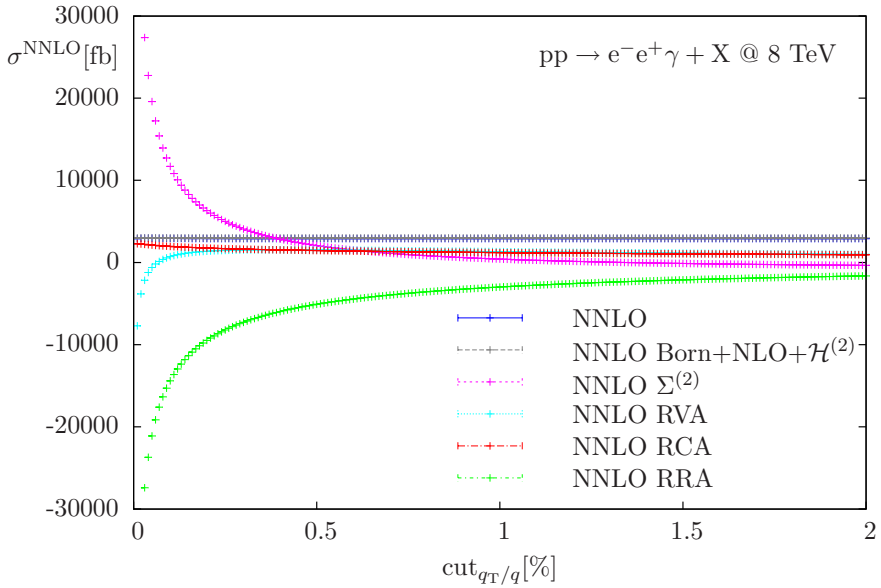

Dependence on q_T (LHC @ 7 TeV, ATLAS setup, $p_{T,\gamma} > 15\,\mathrm{GeV}$)

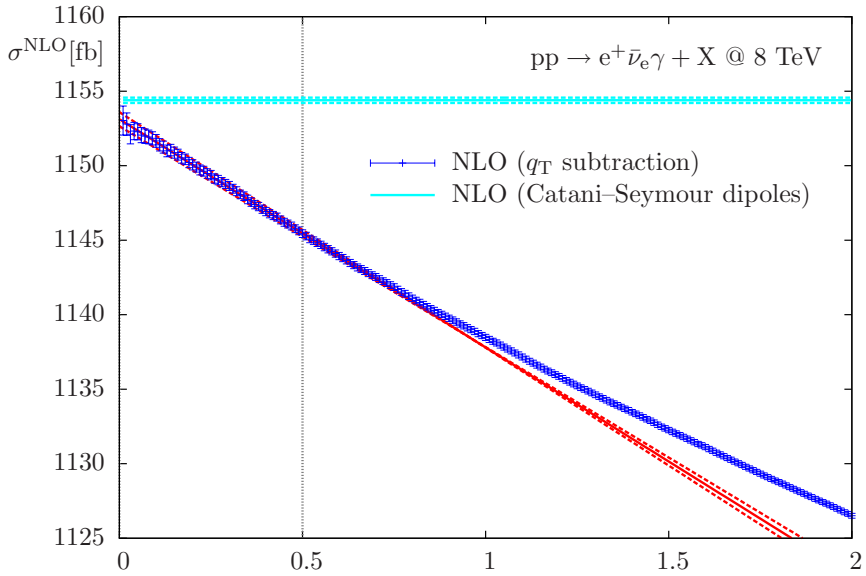

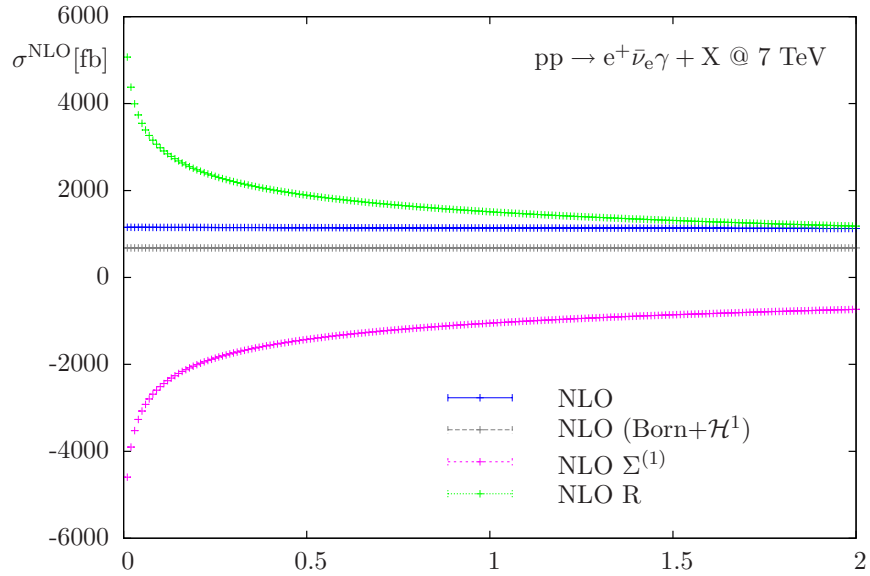

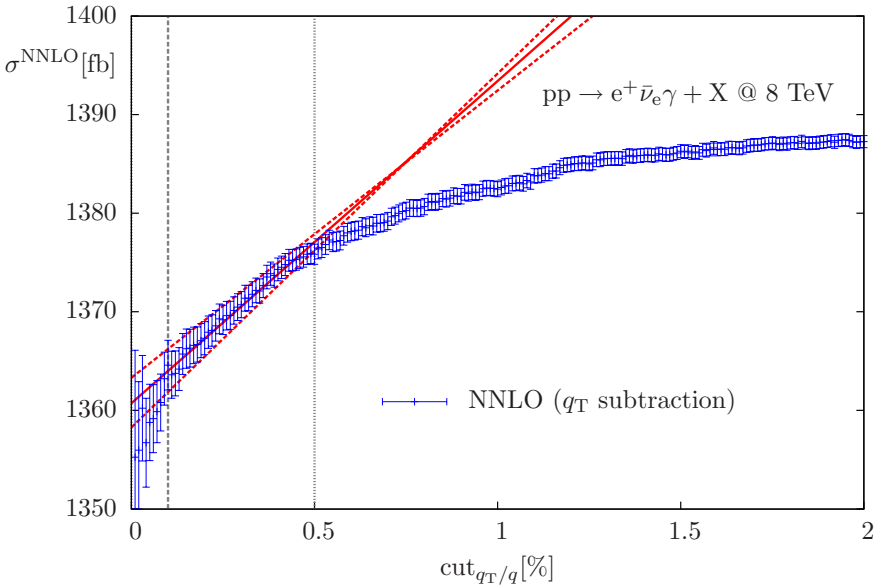

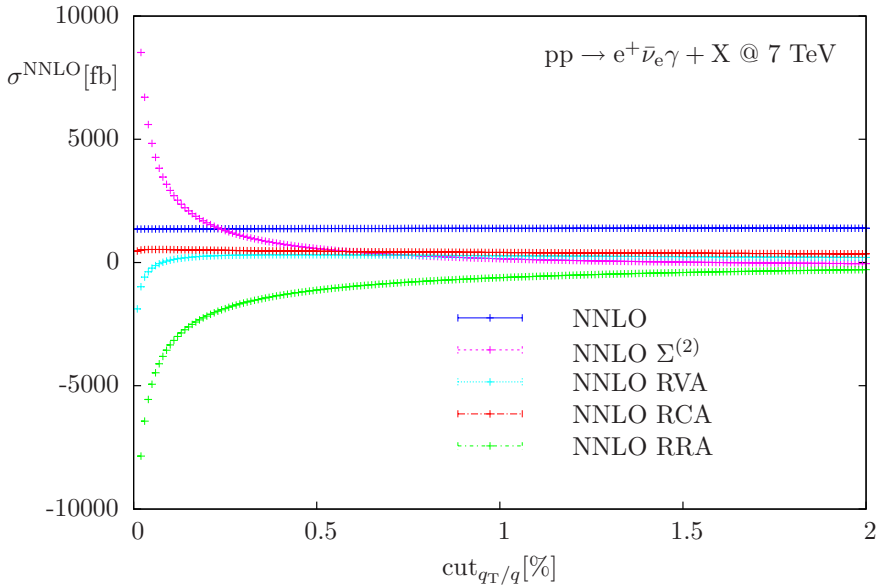

Dependence on q_{T} (LHC @ 7 TeV, ATLAS setup, $p_{\mathrm{T},\gamma} > 15\,\mathrm{GeV}$)

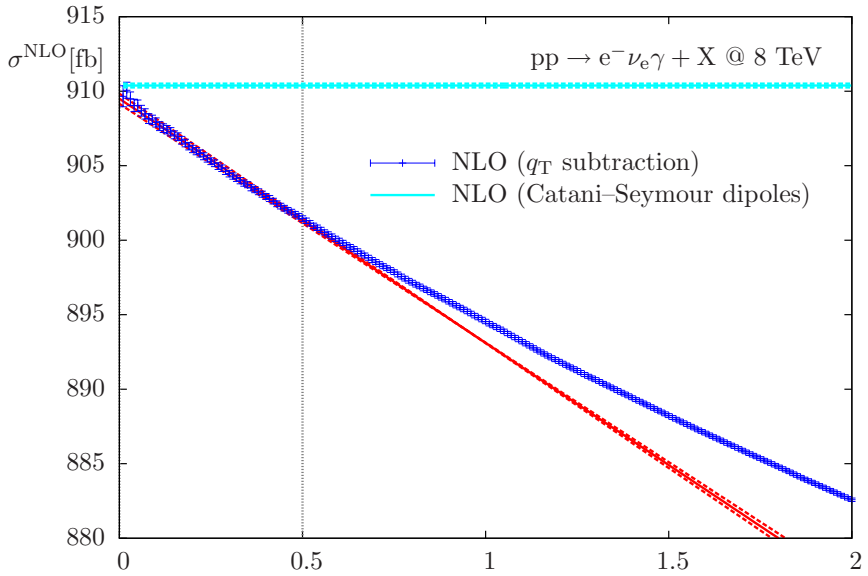

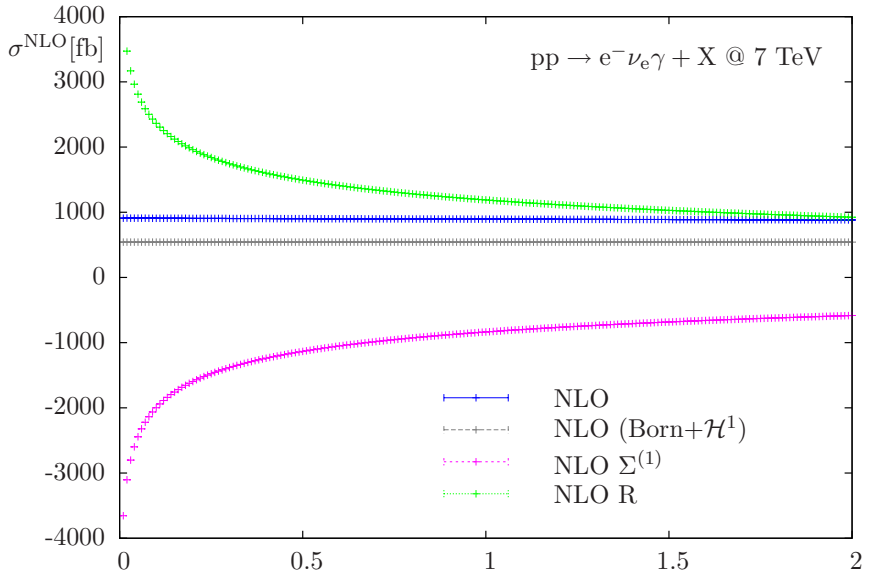

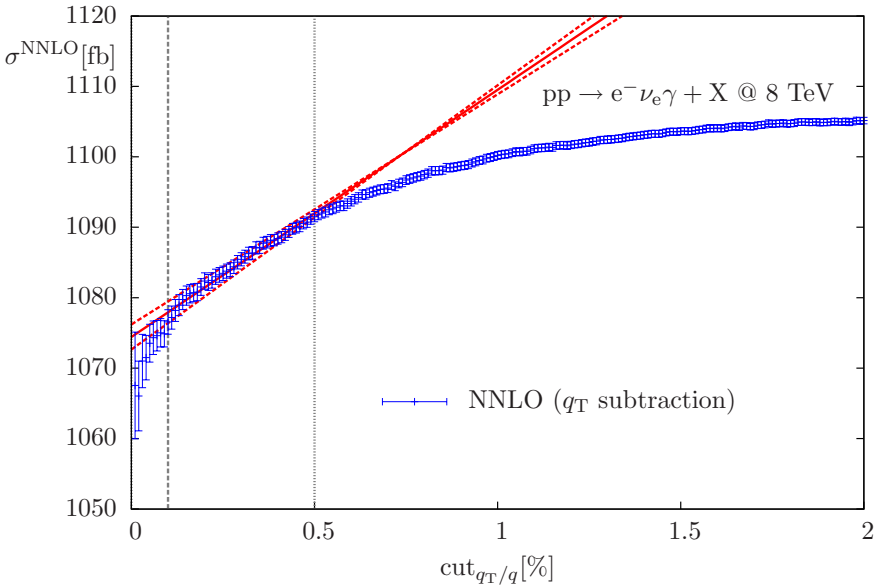

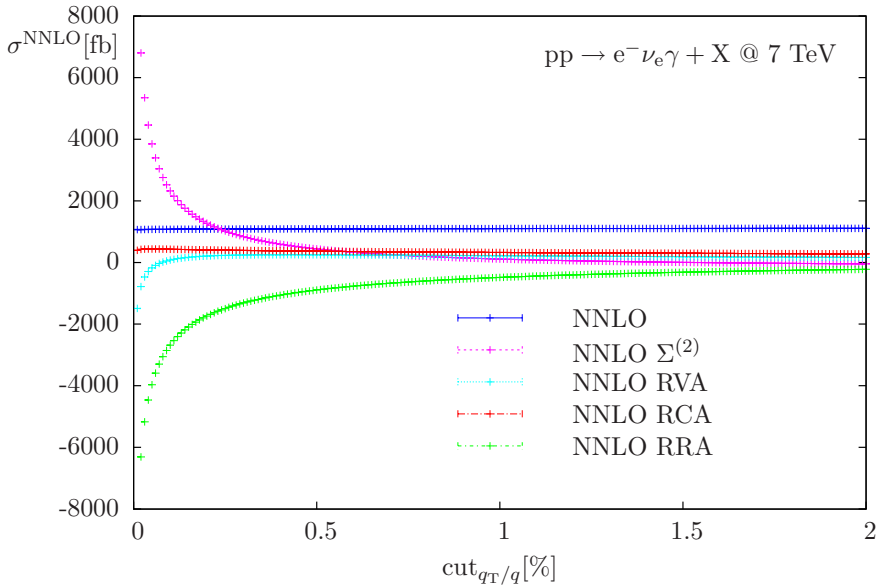

Scale variation (LHC @ 7 TeV, ATLAS setup, $p_{\mathrm{T},\gamma} > 15\,\mathrm{GeV}$)

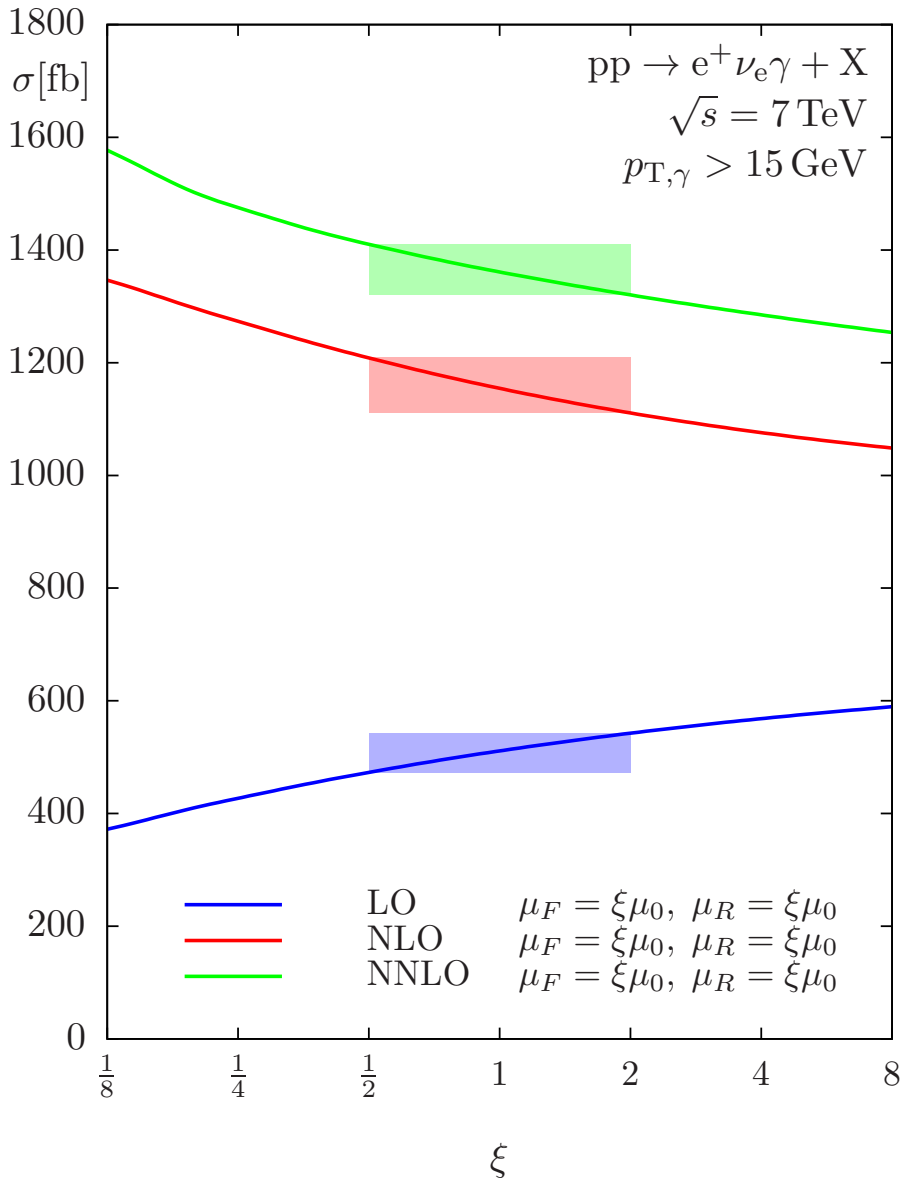

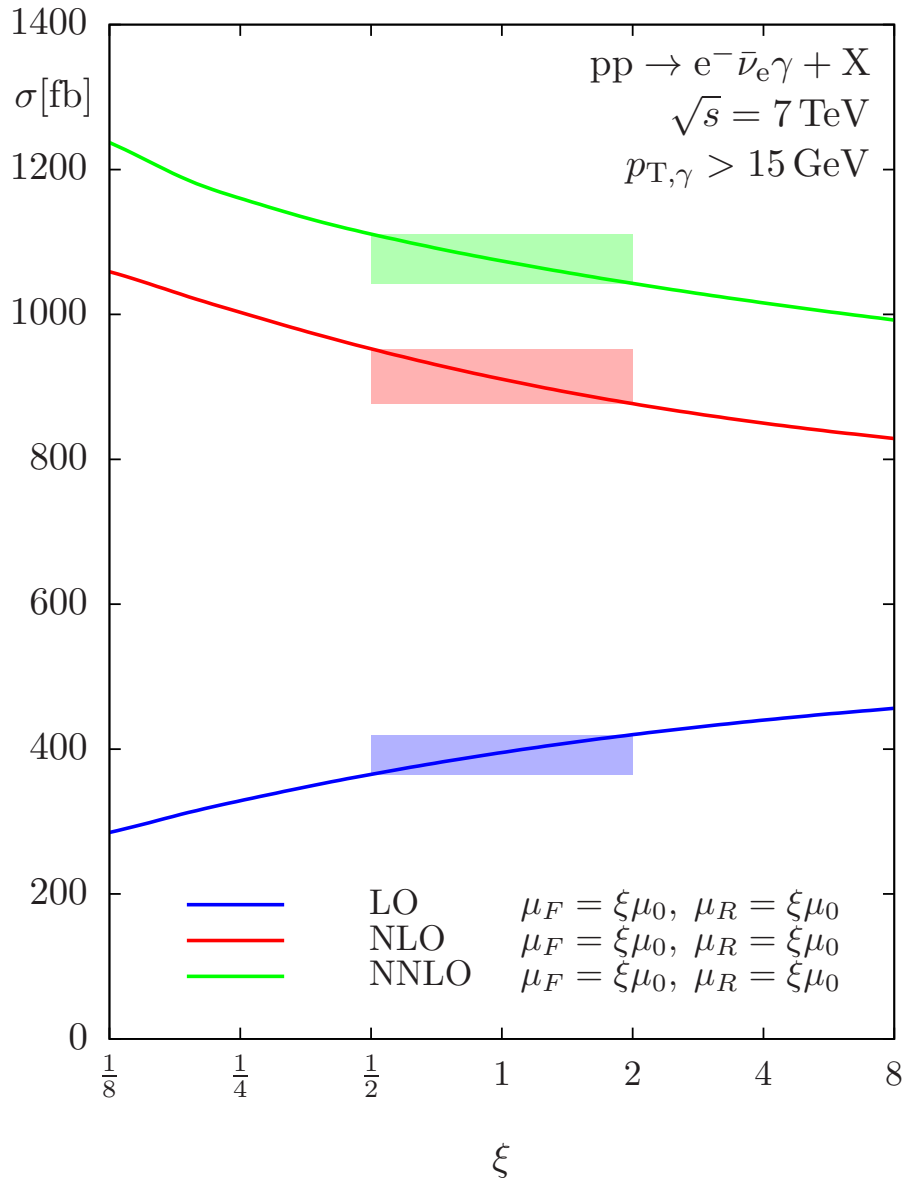

Comparison between $Z\gamma$ and $W^{\pm}\gamma$ results

Considerably larger K factor in $W^{\pm}\gamma$ compared to $Z\gamma$ (ATLAS @ 7 TeV, $p_{T,\gamma} > 15\ GeV$)

	LO	NLO	NNLO	NLO/LO	NNLO/NLO
$Z\gamma$	$0.8507[2]^{+7\%}_{-9\%}$ pb	$1.2262[4]^{+4\%}_{-5\%}$ pb	$1.305[3]^{+1\%}_{-2\%}$ pb	+44%	+6%
$W^+\gamma$	$0.51112[6]^{+6\%}_{-7\%}$ pb	$1.1545[2]^{+5\%}_{-4\%}$ pb	$1.361[6]^{+4\%}_{-3\%}$ pb	+126%	+18%
$W^-\gamma$	$0.39531[4]^{+6\%}_{-8\%}$ pb	$0.9106[2]^{+5\%}_{-4\%}$ pb	$1.074[6]^{+3\%}_{-3\%}$ pb	+130%	+18%

A likely explanation: Breaking of **radiation zero** beyond LO

- $u\bar{d}/d\bar{u} \to W^{\pm}\gamma$ amplitudes vanish at $\cos\theta_{q\gamma,CMS} = \mp 1/3$ [Mikaelian/Samuel/Sahdev (1979)].
- **Radiation zero** leads to a dip at $\Delta y_{l\gamma} = 0$ in pp collisions [Baur/Errede/Landsberg (1994)]:

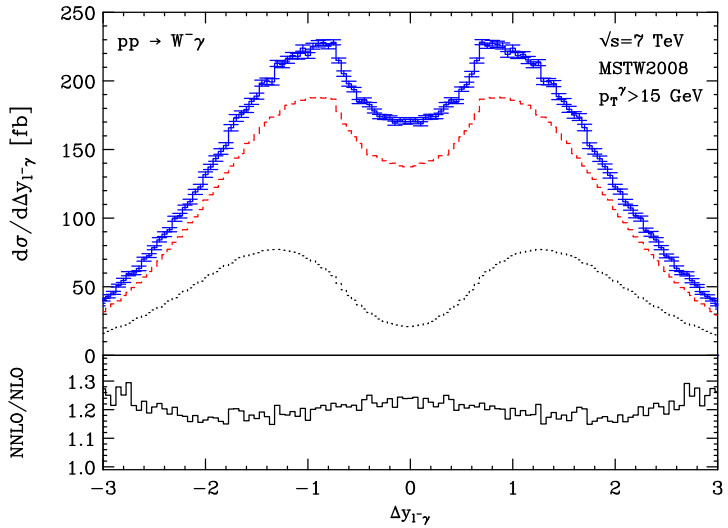

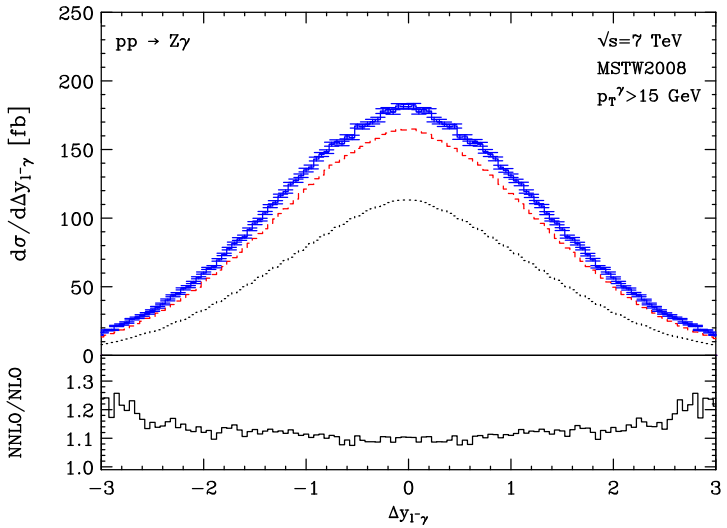

NLO QCD cross section via dipole subtraction

Schematic formula for the NLO cross section in the situation of two initial-state hadrons by means of Catani–Seymour dipoles [Catani, Seymour (1993)]:

$$\sigma^{\mathrm{NLO}} = \underbrace{\int_{m+1} d\sigma^R}_{\text{real corrections}} + \underbrace{\int_m d\sigma^V}_{\text{virtual corrections}} + \underbrace{\int_0^1 dz \int_m d\sigma^C}_{\text{collinear-subtraction counterterm}} - \int_{m+1} d\sigma^A + \int_{m+1} d\sigma^A,$$

$$d\sigma^A = \sum_{\text{dipoles}} d\sigma^B \otimes dV_{\text{dipole}}$$

$$= \int_{m+1} \left[d\sigma^R - d\sigma^A \right]_{\epsilon=0} \qquad \Rightarrow \mathrm{RA}$$

$$+ \int_m \left[d\sigma^V + \sum_{\text{dipoles}} d\sigma^B \otimes V_{\text{dipole}}(1) \right]_{\epsilon=0} \qquad \Rightarrow \mathrm{VA}$$

$$+ \int_0^1 dz \int_m \left[d\sigma^C + \sum_{\text{dipoles}} \int_1 d\sigma^B(z) \otimes [dV_{\text{dipole}}(z)]_+ \right]_{\epsilon=0} \qquad \Rightarrow \mathrm{CA}$$

$$dV_{\text{dipole}}(z) = [dV_{\text{dipole}}(z)]_+ + dV_{\text{dipole}}(1)\delta(1-z)$$

NLO QCD cross section via q_{T} subtraction

Schematic formula for the NLO cross section:

$$\sigma^{\mathrm{NLO}} = \underbrace{\int_{m+1} d\sigma^R}_{\text{real corrections}} + \underbrace{\int_m d\sigma^V}_{\text{virtual corrections}} + \underbrace{\int_0^1 dz \int_m d\sigma^C}_{\text{collinear-subtraction counterterm}}$$

$$= \int_{m+1} d\sigma^R \Big|_{q_{\mathrm{T}}/q \,>\, \mathrm{cut}_{q_{\mathrm{T}}/q}} \qquad \Rightarrow \text{finite, but depends on } \mathrm{cut}_{q_{\mathrm{T}}/q}$$

$$+ \underbrace{\int_{m+1} d\sigma^R \Big|_{q_{\mathrm{T}}/q \,\leq\, \mathrm{cut}_{q_{\mathrm{T}}/q}}}_{\substack{\text{approximated by results known} \\ \text{from } q_{\mathrm{T}} \text{ resummation}}} + \underbrace{\int_m d\sigma^V + \int_0^1 dz \int_m d\sigma^C}_{\substack{\text{identified with corresponding terms} \\ \text{in } q_{\mathrm{T}} \text{ resummation}}}$$

$$\approx \int_{m+1} d\sigma^R \Big|_{q_{\mathrm{T}}/q \,>\, \mathrm{cut}_{q_{\mathrm{T}}/q}} + \frac{\alpha_S}{\pi} \mathcal{H}^{F(1)} \otimes \sigma_{\mathrm{LO}}$$

- no $\mathrm{cut}_{q_{\mathrm{T}}/q}$ dependence,
- contains (finite) 1-loop part.

$$+ \frac{\alpha_S}{\pi} \int_{\mathrm{cut}_{q_{\mathrm{T}}/q}}^{\infty} d(q_{\mathrm{T}}/q) \Sigma^{(1)}(q_{\mathrm{T}}/q) \otimes \sigma_{\mathrm{LO}}$$

- cancels $\mathrm{cut}_{q_{\mathrm{T}}/q}$ dependence,
- assigned to Born phase-space.

NNLO QCD cross section via q_{T} subtraction

Schematic formula for the NNLO cross section:

$$\sigma^{\mathrm{NNLO}} = \underbrace{\int_{m+2} d\sigma^{RR}}_{\text{double-real}} + \underbrace{\int_{m+1} d\sigma^{RV}}_{\text{real–virtual}} + \underbrace{\int_0^1 dz \int_{m+1} d\sigma^{RC}}_{\text{real–collinear}}$$

$$= \sigma^{\mathrm{NLO}}_{F+jet} \Rightarrow \text{at } q_{\mathrm{T}} \neq 0 \text{ calculable via NLO subtraction, but divergent for } q_{\mathrm{T}} \to 0 \Rightarrow \mathrm{cut}_{q_{\mathrm{T}}/q}$$

$$+ \underbrace{\int_m d\sigma^{VV}}_{\text{double-virtual}} + \underbrace{\int_0^1 dz \int_m d\sigma^{VC}}_{\text{virtual–collinear}} + \underbrace{\int_0^1 dz_1 \int_0^1 dz_2 \int_m d\sigma^{CC}}_{\text{double-collinear}}$$

$$= \sigma^{\mathrm{NLO}}_{F+jet}\Big|_{q_{\mathrm{T}}/q > \mathrm{cut}_{q_{\mathrm{T}}/q}}$$

$$+ \underbrace{\sigma^{\mathrm{NLO}}_{F+jet}\Big|_{q_{\mathrm{T}}/q \leq \mathrm{cut}_{q_{\mathrm{T}}/q}}}_{\substack{\text{approximated by results known} \\ \text{from } q_{\mathrm{T}} \text{ resummation}}} + \underbrace{\int_m d\sigma^{VV} + \int_0^1 dz \int_m d\sigma^{VC} + \int_0^1 dz_1 \int_0^1 dz_2 \int_m d\sigma^{CC}}_{\substack{\text{identified with corresponding terms} \\ \text{in } q_{\mathrm{T}} \text{ resummation}}}$$

NNLO QCD cross section via q_{T} subtraction

Schematic formula for the NNLO cross section:

$$\sigma^{\mathrm{NNLO}} = \underbrace{\int_{m+2}\Big[d\sigma^{RRA} + \int_{m+1} d\sigma^{RVA} + \int_0^1 dz \int_{m+1} d\sigma^{RCA}\Big]\Big|_{q_{\mathrm{T}}/q > \mathrm{cut}_{q_{\mathrm{T}}/q}}}_{= \sigma^{\mathrm{NLO}}_{F+jet}\big|_{q_{\mathrm{T}}/q > \mathrm{cut}_{q_{\mathrm{T}}/q}} \;\Rightarrow\; \text{finite, but dependends on } \mathrm{cut}_{q_{\mathrm{T}}/q}}$$

$$+\left(\frac{\alpha_S}{\pi}\right)^2 \mathcal{H}^{F(2)} \otimes \sigma_{\mathrm{LO}}$$

- no $\mathrm{cut}_{q_{\mathrm{T}}/q}$ dependence,
- contains (finite) 2-loop part.

$$+\left(\frac{\alpha_S}{\pi}\right)^2 \int_{\mathrm{cut}_{q_{\mathrm{T}}/q}}^{\infty} d(q_{\mathrm{T}}/q)\Sigma^{(2)}(q_{\mathrm{T}}/q) \otimes \sigma_{\mathrm{LO}}$$

- cancels $\mathrm{cut}_{q_{\mathrm{T}}/q}$ dependence,
- contains (finite) 1-loop part,
- assigned to Born phase-space.

All relevant ingredients from q_{T} resummation ($\mathcal{H}^{F(i)}$, $\Sigma^{(i)}(q_{\mathrm{T}}/q)$ for $i \leq 2$) are known.

↪ Direct implementation into a Monte Carlo integrator feasible.